

DIRIGO/TR-95/01

# DEMONSTRATION OF THE PRODUCTION OF 60 HZ AC POWER DIRECTLY FROM HIGH FREQUENCY ALTERNATORS

Christopher N. Tupper

Dirigo R&D

1995

U.S.ARMY CECOM

19990202 015

SECURITY CLASSIFICATION: UNCLASSIFIED

Approved for Public Release; Distribution Unlimited

DTIC QUALITY INSPECTED 2

REPORT DOCUMENTATION PAGE	1. REPORT NO.	2.	3. Recipient's Accession No.
4. Title and Subtitle Demonstration of the Production of 60 Hz AC Power Directly from High Frequency Alternators			5. Report Date September 1995
7. Author(s) Christopher N. Tupper			8. Performing Organization Report No. DIRIGO/TR-95/01
9. Performing Organization Name and Address Dirigo R&D 14 Industrial Parkway Brunswick, Maine 04011			10. Project/Task/Work Unit No.
12. Sponsoring Organization Name and Address US ARMY CECOM C4IEW ACQ CTR-GROUND SUPPORT BR 10109 GRIDELY ROAD, SUITE 200 FT. BELVOIR, VA 22060-5845			11. Contract(G) or Grant(G) No. (C) DAAB12-95-C-0011 (G)
15. Supplementary Notes			13. Type of Report & Period Covered Contractor Final Report
14. Abstract (Limit: 200 words) This document presents the results of a project to demonstrate the production of 60 Hz AC power directly from high frequency alternators. A technique of modulating the output of existing truck and automotive style DC alternators was developed to produce low voltage single phase 60 Hz rectified output. The load was connected to this source by a commutation circuit that switched polarity of the load at the zero voltage crossing of each half cycle, exciting the load with a sinusoidal waveform. Existing low voltage DC alternators exhibited very high core losses in the 60 Hz modulation of the magnetic field, but calculations show that this could be significantly reduced by use of laminated electrical steel for the entire magnetic circuit. Calculations show that high frequency alternators could be designed to produce 120 VAC directly with low core losses, making this a practical method of generating 60 Hz AC power.			
17. Document Analysis a. Descriptors  b. Identifiers/Open-Ended Terms Power Generation High Frequency Alternators 60 Hz AC Power Tactical Power c. COSATI Field/Group			
18. Availability Statement		19. Security Class (This Report) Unclassified	21. No. of Pages 65
		20. Security Class (This Page) Unclassified	22. Price

(See ANSI Z39.18)

See Instructions on Reverse

OPTIONAL FORM 272 (4-77)

\* GPO : 1983 O - 381-526 (8393)

**DEMONSTRATION OF THE PRODUCTION OF 60 HZ AC POWER  
DIRECTLY FROM HIGH FREQUENCY ALTERNATORS**

**ABSTRACT**

This document presents the results of a project to demonstrate the production of 60 Hz AC power directly from high frequency alternators. A technique of modulating the output of existing truck and automotive style DC alternators was developed to produce low voltage single phase 60 Hz rectified output. The load was connected to this source by a commutation circuit that switched polarity of the load at the zero voltage crossing of each half cycle, exciting the load with a sinusoidal waveform. Existing low voltage DC alternators exhibited very high core losses in the 60 Hz modulation of the magnetic field, but calculations show that this could be significantly reduced by use of laminated electrical steel for the entire magnetic circuit. Calculations show that high frequency alternators could be designed to produce 120 VAC directly with low core losses, making this a practical method of generating 60 Hz AC power.

## CONTENTS

ABSTRACT . . . . .	ii
FIGURES . . . . .	iv
1 SUMMARY . . . . .	1
2 INTRODUCTION. . . . .	3
3 DEVELOPMENT PROCEDURE . . . . .	8
4 DISCUSSION OF RESULTS . . . . .	28
5 CONCLUSIONS . . . . .	40
APPENDIX A: Detailed Circuit Diagrams. . . . .	42
APPENDIX B: Calculation for Sketch Design. . . . .	48
APPENDIX C: Outline of Coreloss Estimation Procedure . . . . .	59

# LIST OF FIGURES

<u>FIGURE</u>	<u>TITLE</u>	<u>PAGE</u>
1	Schematic of Typical of High Frequency Alternator	4
2	Modulated Output of High Frequency Alternator	5
3	Schematic of Commutation Scheme with Waveforms	6
4	Typical Field Drive Circuit	9
5	Alternator Control Loop Circuit	10
6	Alternator Output Ripple	11
7	Armature Filter Circuit	12
8	Resonant Drive with Transformer Coupling	15
9	Open Loop Circuit for 60 Hz Modulation	15
10	Field Coil Excitation Waveforms	16
11	Commutation Circuit and Schematic Waveforms	19
12	Schematic of High Side Switch	20
13	Alternate Commutation Scheme with Twelve SCRs	21
14	Test Set Up for Gated SCR Commutation Trials	22
15	Reaction Branch Circuit	23
16	Modified Reaction Branch with Sense Diode	24
17	Schematic of Field and Armature Coil Arrangement in Sketch Design	25
18	Magnetic Path Entirely of Laminated Steel for Sketch Design	26
19	Waveforms of a High Frequency Alternator Driving a 75 ohm Load with 60 Hz AC Power	28
20	Typical Alternator Magnetization Curve	30
21	100 Ohm Load: Modulated Output of Alternator at 60 Hz	33
22	1 Ohm Load: Modulated Output of Alternator at 60 Hz	33
23	60 Hz Field Excitation Waveforms for Figure 22	34
24	60 Hz Field Excitation Waveforms for ZERO RPM	35
25	Commutation	36
26	Reactive Loads: Waveforms with Reactive Branch	37
A-1	High Level Schematic: Power and Control Circuits	42
A-2	Power Circuit Circuit	43
A-3	Phase and Sense Control Circuit	44
A-4	Low Side Drivers	45
A-5	High Side Drivers	46
A-6	Reaction Sense and Control Circuit	47
B-1	Air Gap Area Variations	48
B-2	Armature Coil - Voltages	50
B-3	Flux Variations	54
B-4	Sketch of Pole Core Dimensions	56
C-1	Time Modulation of Core Flux for Sketch Design	59

**DEMONSTRATION OF THE PRODUCTION OF 60 HZ AC POWER  
DIRECTLY FROM HIGH FREQUENCY ALTERNATORS**

**1. SUMMARY**

This project successfully demonstrated a novel approach to generating 60 Hz AC power directly from the output of high frequency alternators. The technique involved 60 Hz modulation of the field current and thus the magnetic intensity within the alternator. This led to a rectified 60 Hz output with a high frequency ripple which came from the normal rectification of the three phase high frequency output of the alternator. The alternator output was then unfolded from the rectified 60 Hz sine wave into a normal sine wave by an active bridge circuit that commutated the load at the end of each half cycle (zero crossing of the output.)

The project also demonstrated the use of a low impedance shunt branch actively switched in and out of the circuit as needed to handle reactive loads that could not be accommodated by the rectified nature of the alternator output. The reactive branch low impedance shunt allowed capacitive and inductive loads to see a low impedance source during the portions of each cycle that they needed to "return" stored energy. This energy was dissipated in the shunt branch, rather than stored and reused, but this technique allowed the reactive loads to be excited by near sinusoidal waveforms.

It was found that existing automotive and truck style alternators absorb and dissipate a great deal of power when modulated at 60 Hz. This energy is lost in hysteresis and eddy current losses, or core losses, in the magnetic field. The existing alternators, being designed for DC operation, have at least part of their magnetic circuits made of solid core iron or steel. When the magnetic field is modulated at 60 Hz a great deal of energy is lost to eddy currents in the solid sections of the core.

In the demonstrations using existing automotive and truck alternators the field excitation absorbed 307 watts of active 60 Hz AC power while the alternator's 60 Hz AC output was 50 volts peak to peak into 75 ohms, or 30 volts peak to peak into 1 ohm. The maximum output power was 137 watts. The demonstrations made it clear that the field absorbs more 60 Hz electrical energy than is produced by the device. It is impractical to use existing alternators for generating 60 Hz AC power.

Theoretical analysis suggests that with the use of a magnetic path made entirely of laminated electrical steel, the field losses can be made to be trivial. The analysis suggests that the low voltage output of existing alternators can be scaled up to 120 VAC and the losses can be minimized so that generating AC power by this method becomes practical and attractive.

Commutation of the load was accomplished using a typical H-Bridge arrangement. Preliminary investigations were made into the feasibility

of using a alternative commutation system that eliminated this H-Bridge and its silicon losses. The alternative replaces the normal six rectification diodes with twelve SCR's. The alternative approach has numerous potential benefits and the initial results were promising.

The system has been demonstrated to be possible. The calculations suggested that it can be made very practical and attractive. The next logical step is the construction of an engineering prototype of a scaled up alternator producing 120 VAC directly. This prototype would be used to verify the expected dramatic reduction of core losses through the use of laminated materials in the magnetic path.

## 2. INTRODUCTION

2.1 General The availability of 60 Hz AC power is important for some mobile and field site applications for both military and commercial use. The traditional approaches to providing this power have been the use of small synchronous generators, or the use of power electronic inverters or high frequency power conversion technology (frequency changers.) Each approach has distinct advantages and disadvantages. The synchronous generators are simple and provide a clean low impedance power source, but require a dedicated fixed speed engine drive and are relatively heavy. Inverters take the DC output of speed independent, high frequency alternators and use power electronics to switch and control the load current to mimic 60 Hz AC power; this adds complexity, inefficiency and noise to the system. Power frequency changers are similar but replace the DC rectification step by switching in the momentarily desired portion of the alternator's natural high frequency AC output in order to reconstruct the desired 60 Hz AC waveform.

This project demonstrates a novel approach for providing 60 Hz AC power directly from alternators by modulating the alternator output at 60 Hz. This is accomplished by 60 Hz AC modulation of the field excitation. In conjunction with the natural commutation of the usual rectification diodes, this approach will produce a rectified 60 Hz output. This output can then be further unfolded into a sine wave by commutating the load. That is, for the first half cycle one end of the load is switched to ground, and the other end is connected to the modulating (rectified) output of the alternator. As the modulated output voltage approaches zero at the end of the half cycle, each end is switched to the opposite pole. Therefore, during the second half cycle the opposite end is connected to ground, etc, and the current flows the opposite direction through the load. Effectively the load is swapped end-for-end at each half cycle. This subjects the load to sinusoidal excitation.

There are several possible benefits of this approach compared to the other approaches. Like the inverter and power frequency changer it utilizes a high frequency alternator instead of the slow, relatively heavy synchronous generator. This means 60 Hz AC power can be produced while the driving engine can operate at its most efficient speed for its overall task. Two major benefits are that this can save fuel, or allow the AC power generation to be incidental to the operation of a prime mover. It can also make the system lighter, which is important in mobile and field applications. In contrast to the inverter or the power frequency changer, this approach shapes and modulates the small field currents rather than the full load current. This can reduce the size, complexity and inefficiency of the power electronics employed. This approach makes use of the fact that the electronic modulation in the small power electronics of the field are essentially amplified by the inherent mechanical arrangement of the alternator. This approach allows more power to be controlled with smaller electronics, leveraging the state of the art.

Commutation of the load is done at zero volts, making for soft switching. This method does not inherently generate harmonics of the fundamental 60 Hz output. It has the potential for a good sine wave



output, complicated only by high frequency ripple which is relatively easy to filter.

**2.2 Background** Existing truck and automotive alternators commonly generate three phase AC power at relatively high frequency. These frequencies are not precisely controlled but range from 300 to 800 Hz depending upon the engine speed of the moment. This three phase AC power is then rectified with diodes to produce "DC" power as shown in Figure 1. The phase voltage waveforms are also shown in Figure 1 along with the rectified output voltage with one bus is held at ground. Note the hex phase ripple voltage at six times the fundamental phase frequency. This ripple varies from  $(1.5)V_p$  to  $(1.78)V_p$ , where  $V_p$  equals peak voltage per phase.

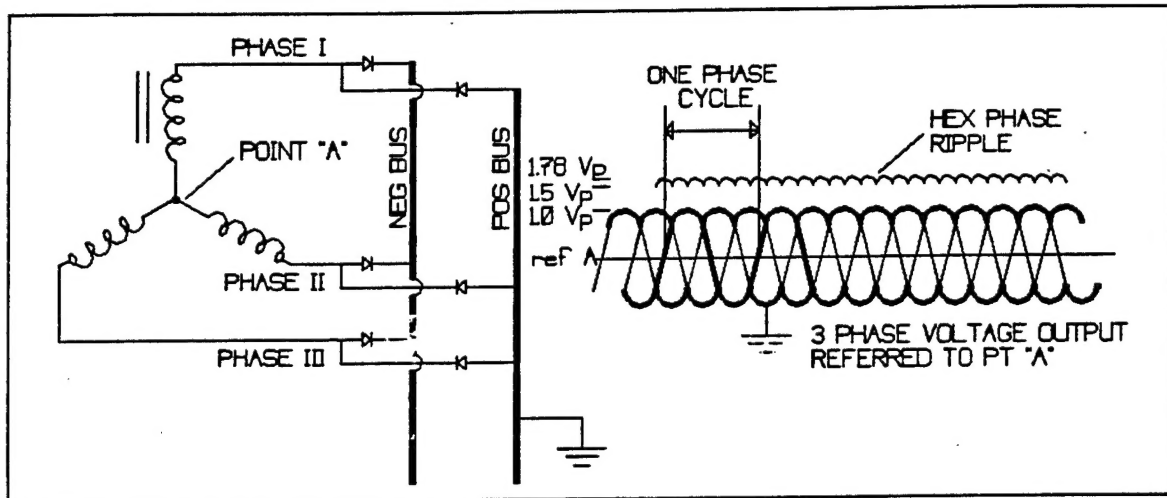


**FIGURE 1**  
Schematic of Typical High Frequency Alternator with Waveforms

As suggested in Figure 1 the output of the alternator is controlled by the current in the field coil, which establishes the level of magnetic intensity within the machine. The magnetic field is then caused to change by shaft rotation, either by physically rotating the field or by physically changing the reluctance of the magnetic circuit through the opening and closing an air gap. This high frequency physical manipulation of the magnetic field causes the high frequency AC electrical output.

The general scheme of this project involves adding an electrical modulation of the magnetic field by varying the current in the field coil at 60 Hz. This will change or modulate the DC output of Figure 1 and produce the rectified output shown in Figure 2. Note that the high frequency ripple is still present.

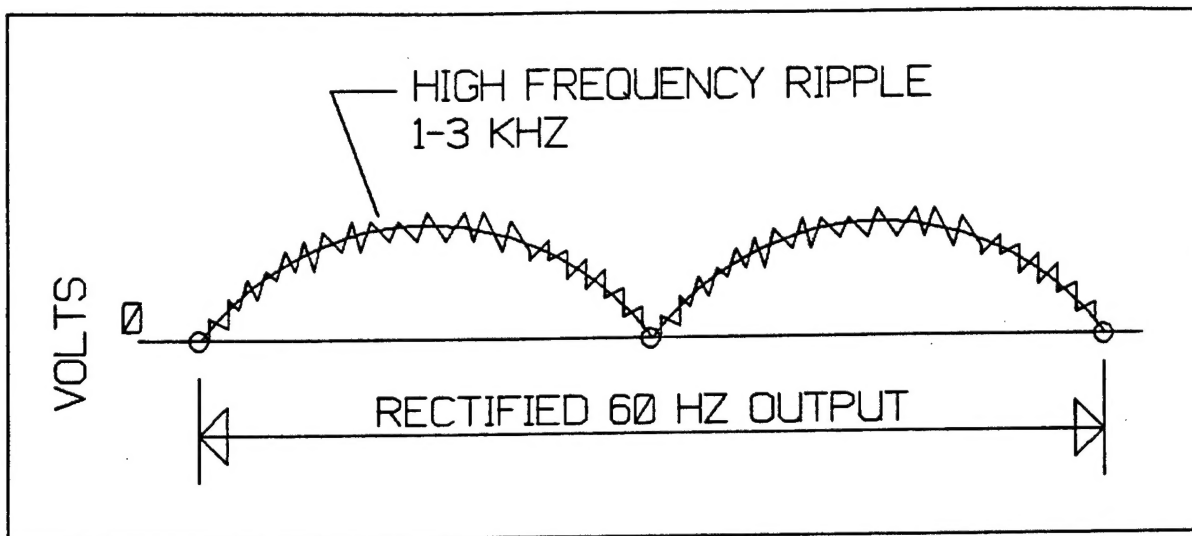


**FIGURE 2**

**Modulated Output of High Frequency Alternator to Provide Rectified 60 Hz Waveform.**

The second step in this scheme is to apply the modulated rectified output shown in Figure 2 to a load through a switching circuit that commutates the load on each half cycle of the rectified output. Figure 3 shows a simple H-Bridge with MOSFET switches that can provide such commutation. Switches are activated in diagonal pairs, (1 and 3) or (2 and 4). When switches (1 and 3) are on, the current flows through the load from A to B as shown. As the driving voltage from the alternator is modulated to zero, the switches (1 and 3) are shut off and switches (2 and 4) are turned on, reversing the polarity of the load and the direction of the current. From the waveform sketch it can be seen how load is subjected to a single phase sinusoidal voltage.\* Other commutation schemes are possible.

\* Note: The ground point shown in Figure 3, while convenient for controlling the alternator, is arbitrary. One end of the load (such as point B) could be established as ground (which is more traditional) and then the alternator would become a "floating" source. The scheme would still work.

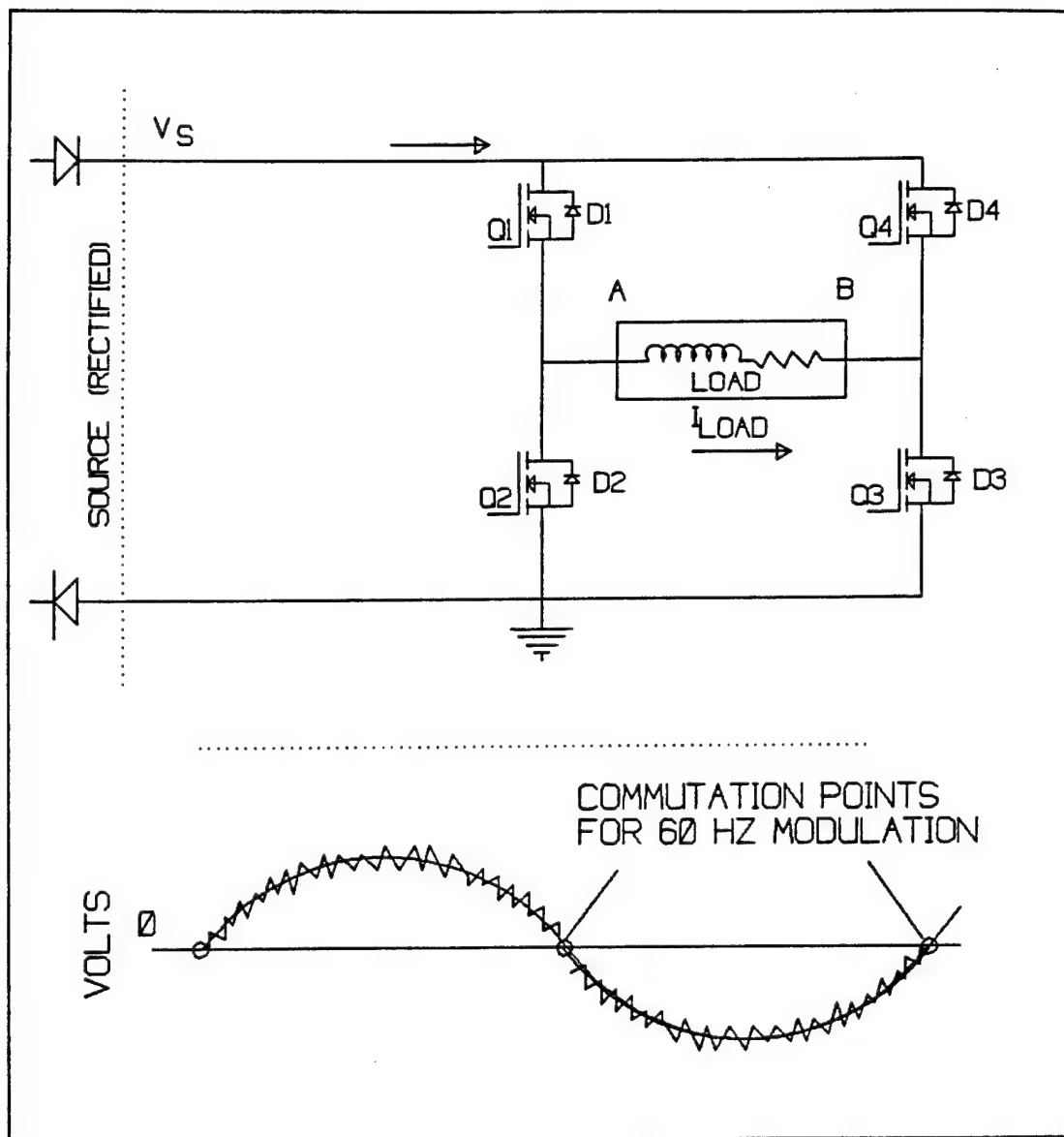


**FIGURE 3**  
Schematic of Commutation Scheme with Waveforms

These two concepts, modulation of the output and commutation of the load, form the basis for the scheme investigated in this project. Although the technique is simple, it is only relatively recently that power electronics have evolved to allow such an approach.

**2.3 Purpose and Scope** This project explored and demonstrated the production of 60 Hz AC power directly from existing (low voltage) high frequency alternators. The project used 60 Hz modulation of the field to induce modulation of rectified the output for existing truck and automotive style alternators. This modulated output was then connected to a load with a commutating circuit to provide the load with (low voltage) 60 Hz AC excitation.

This project also addressed the issue of handling reactive loads from a rectified source. The rectified source will not accept the return of energy stored in the reactive load. This disrupts the sinusoidal flow of current and power in and out of the load. Solutions to this complication were explored.

Since existing high frequency truck and automotive alternators are designed for low voltage (12-32v), this project addressed the theoretical potential for scaling the alternator designs to produce 120 VAC power. It also addressed the issues of suitability of the present design of these alternators for the proposed use.

2.4 Presentation Section 3 presents a review of the development effort highlighting some of the unexpected findings and alternative approaches that were used as the developmental aspects of the project unfolded. Section 4 discusses the results particularly as they relate to the objective of demonstrating the production of 60 Hz AC power from the existing alternators. Section 5 presents the conclusions. Appendix A presents the power and control circuits used to demonstrate the combined modulation, commutation and handling of reactive loads. Appendix B presents the details of the "sketch design" calculations for a 6 kW, 120 VAC, alternator producing 60 Hz power. Appendix C details the assumptions used in calculating magnetic core losses.

### 3. DEVELOPMENT PROCEDURE

3.1 Approach Overview This development project used existing truck and automotive high frequency alternators, designed to provide low voltage DC power through rectification, to demonstrate the feasibility of producing low voltage 60 Hz AC power\*. The normal field excitation circuits were replaced with special drive circuits to modulate the alternator's rectified output at 60 Hz. The load was then commutated (swapped end for end) by an external circuit at every half cycle. This commutation unfolded the rectified wave back into a full sine wave. The development procedure was broken into a series of independent steps:

- Development of tight regulation.

- Development of modulation of output

- Development of commutation of load

- Development of handling reactive loads

- Analytical development of future improvements (such as 120 VAC)

Finally the modulation and commutation were used together to demonstrate the production of 60 Hz AC power from the high speed alternator. The text of this report follows through each of these development steps in order.

Because this was a development project, various approaches were tried which led to unexpected results and which suggested alternate approaches. These unexpected results and the rationale for alternative approaches are discussed in this section. Detailed results of the 60 Hz AC performance of the system are discussed in Section 4, "Discussion of Results."

3.2 Development of Tight Regulation Typically automotive and truck alternator have a voltage regulator that excites the field to provide a steady (DC) output. The current in the field coil establishes the magnetic field intensity in the alternator and controls the alternator output voltage. The usual regulator was replaced with a similar closed loop controller that could be made follow an external reference.

Preliminary tests were made of the time constant of the field coil situated in its place in the magnetic circuit of the alternator, with the alternator not running. The field coil drive circuit was the typical single sided drive; a coil with free wheeling diode gated to ground through a transistor as shown in Figure 4. The transistor duty cycle is typically controlled by a pulse repetition rate or pulse width modulation control; the latter was used in this project. The time constants were measured by noting the step response time as the transistor was turned on or off. The coil would charge through the transistor, which gave one time constant. When the transistor was shut off, the coil would discharge through the free wheeling diode; this gave a shorter time constant due to the extra energy absorbed by the diode. The inductance as inferred from the longer time constant and the measured DC resistance of the coil.

---

\* NOTE: Alternators are generally three phase machines. These three phases of high frequency power are usually rectified by natural commutation into DC power. The thrust of this development effort was to modulate and commute the rectified "DC" into a single phase of 60 Hz AC power.

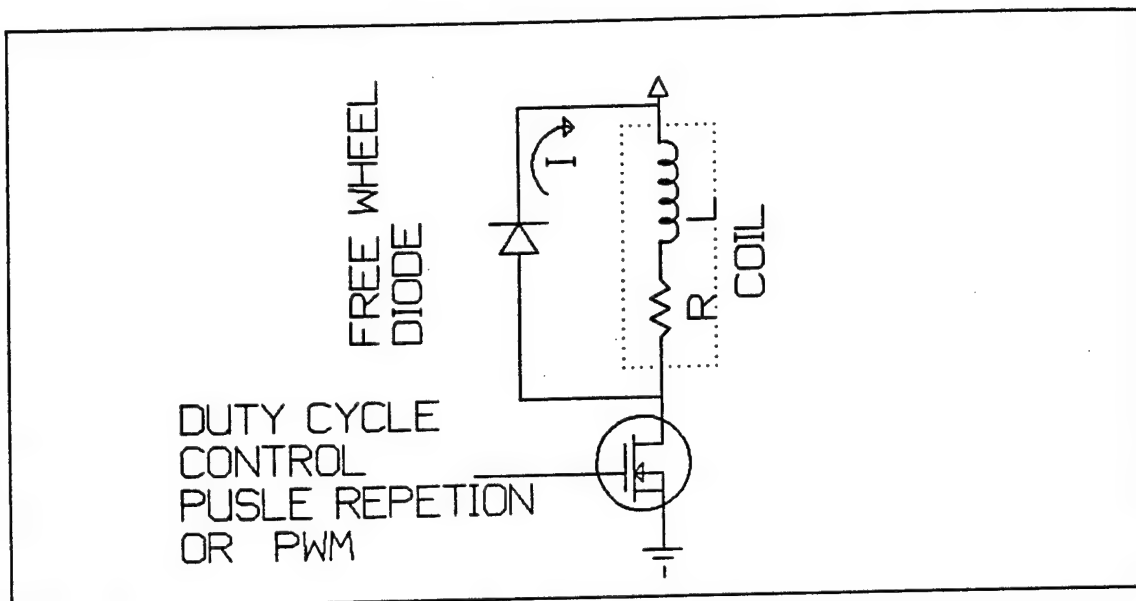


**FIGURE 4**  
Typical Field Drive Circuit

The initial tests were done on an Electrodyne brand heavy duty, brushless, alternator rated at 32 volts (V) DC and 100 amps (A). This unit, of unique design, will be referred to as "truck style" to differentiate it from the more usual automotive style alternator used later in the project. This alternator was loaned to this project by Gauss Corporation of Scarborough., Maine. The coil of this unit showed a time constant of 0.45 seconds and a resistance of 13 ohms, from which an inductance of about 6 henries (H) was inferred. This indicated that the coil had a pole frequency of about 0.35 hertz (Hz), which is far too slow for 60 Hz modulation. This indicated that tremendous voltages would be required to modulate the current flow in the coil at 60 Hz.

In the tight regulation tests, the alternator was enclosed in a closed loop feedback controller as shown in Figure 5. The alternator shaft was driven by an electric motor and belt drive at nominal speeds of 3219 and 5382 RPM. Initial plans were for a control unit using a single sided field drive circuit and trying to follow a rectified reference signal, as shown. This worked fine for slow speed variation of the reference signal. With modest driving voltages it was possible to get limited 60 Hz fluctuation riding on top of a DC output level. It was clear that the field coil inductance was too high for meaningful amounts of 60 Hz modulation. (High inductance is good for DC operation since high inductance means a lot of magnetic energy stored per amp of field current, making the unit very efficient.)

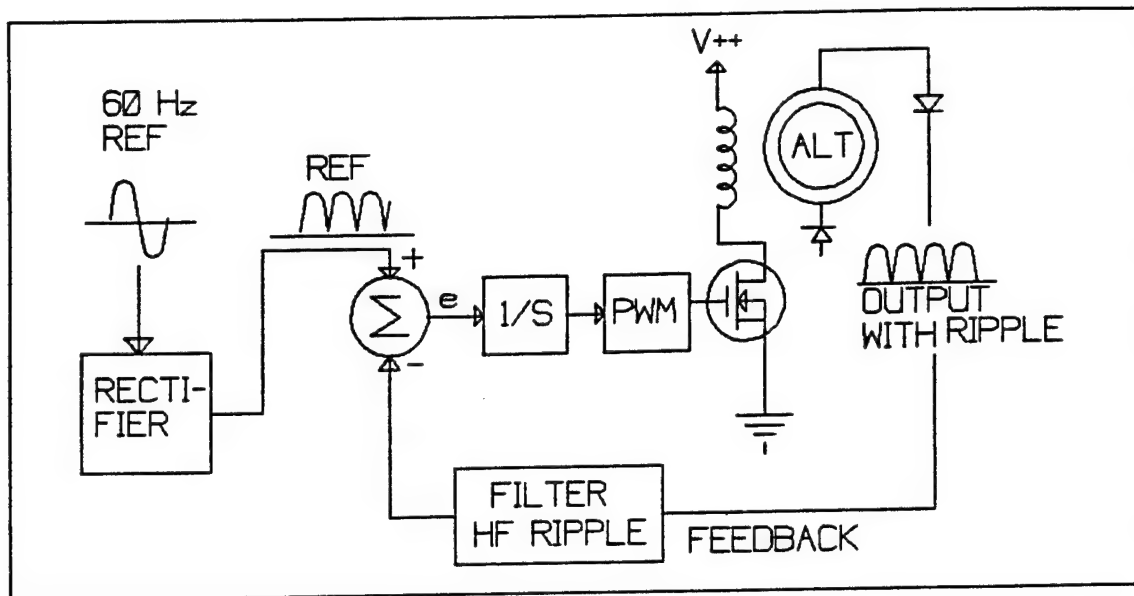


FIGURE 5

Alternator Control Loop Circuit

The truck style alternator output had an unexpectedly high ripple output. This output is shown in Figure 6 where the excessive ripple of the truck style alternator (left) is compared with the ripple output of an automotive style alternator (right.) The ripple frequency did not show the hex phase pattern expected from three phase sine waves and natural commutation. (Compare with Figure 1.) The observed ripple was one half the frequency and many times the magnitude expected. This is due to the geometry of the truck style alternator's rotor and stator. Such excessive ripple is not of great importance in DC systems where the battery acts as a very large capacitor and filters out the ripple. For 60 Hz AC operation, however, this ripple is too large and too close to the 60 Hz frequency to be filtered out. In the initial tests the ripple frequency was about 1200 Hz.

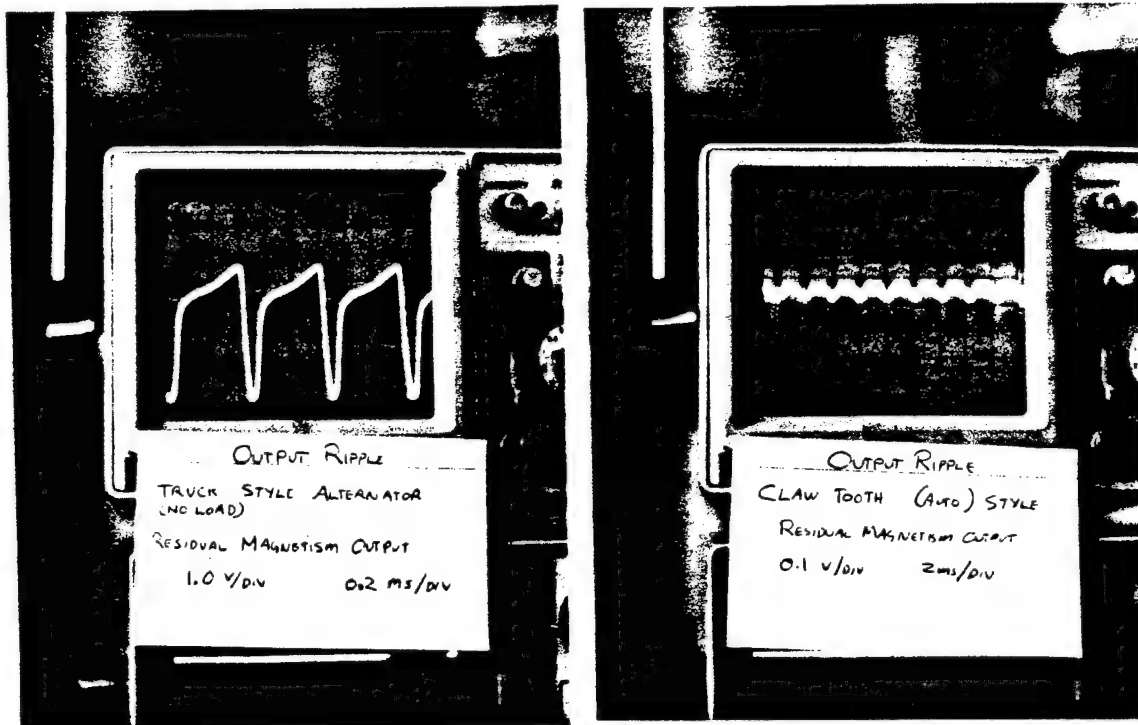


FIGURE 6

Alternator Output Ripple  
 Left: Truck Style Alternator 1.0 V/div - 0.2ms/div  
 Right: Automotive Style Alternator, 0.1 V/div - 2.0ms/div  
 Both Traces: 0 V DC at bottom of screen  
 (Residual Magnetism Excitation)

An attempt was made to filter out the ripple by filtering at the armature coils before the rectification diodes. This scheme is shown in Figure 7. Capacitors were added in a delta connection in parallel with the Wye connection of the phase coils. This provided a much smoothed output with a ripple frequency still half that expected from hex phase rectification. The average output voltage was about one half that from the unfiltered configuration. The amperage consumed by the motor driving the alternator increased considerably.



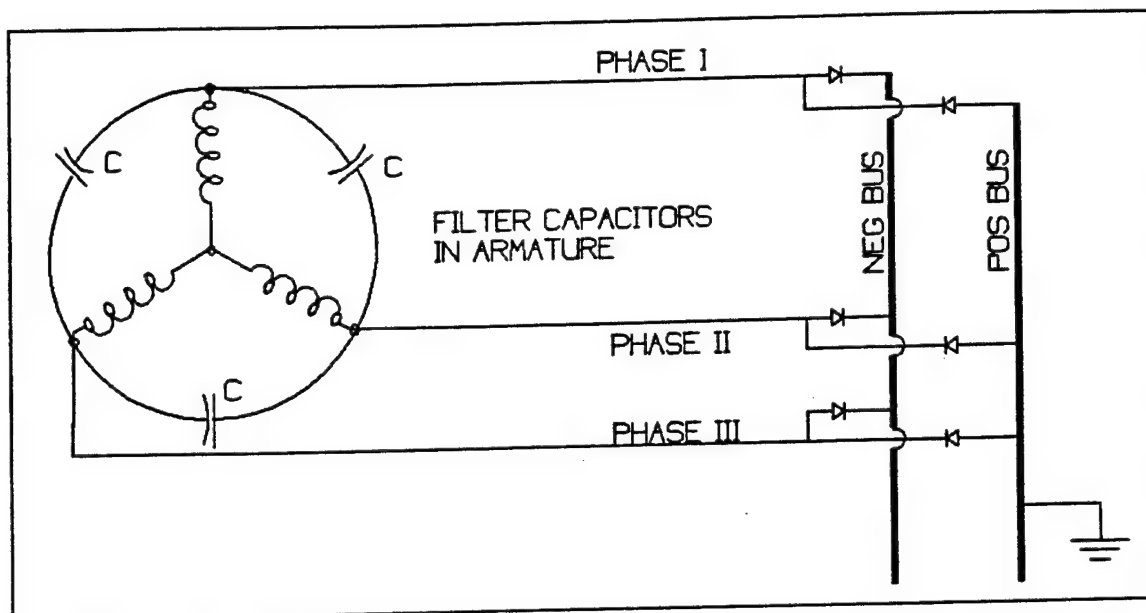


FIGURE 7

#### Armature Filter Circuit

The "magnetization currents" were explored by the development of magnetization curves, with and without the armature filters, and with various loads. This was done by driving the field coil with various DC currents and noting the output voltage. This was done with quasi-static exciting currents that were slowly stepped up and down. When the output voltage was plotted against the electro-motive force (MMF in amp turns), the results showed the hysteretic nature of the magnetization curves. There was substantial residual magnetism evident. Usually the unexcited alternator could produce 1-5 volts of output just from its residual magnetism. The exact value depended upon the load and the previous level of magnetization.

Since the proposed scheme involved modulating the output to zero volts as part of the rectified 60 Hz output, the demagnetization curves were explored by reversing the field current and watching the output voltage reduce. Approximately 50 amp turns of MMF were required to counter the residual magnetism and bring the output to zero. As expected, additional reverse current led to a rise in the output voltage because of the rectification of the output.

With increasing load current the output voltage would drop. Attempts were made to model this as a reverse MMF from the load current, reducing the magnetic field strength and thus the output. These models were not consistent with the data. A model of an internal resistance of about 1 ohm in the load circuit more accurately described the performance of the alternator. Interestingly, the alternator with the filtered armature circuit showed no change in output with load; the filtering effect masked the load effects.

In an attempt to increase the output voltages from the filtered alternator, the drive speed of the alternator was increased by a change in the sheave diameters. This put the filter circuit of Figure 7 into a resonant mode. Output ripple showed the expected characteristics of hex phase rectification. The output voltage rose dramatically. Without any field excitation, the residual magnetism drove the alternator's rectified output to 249 volts DC with no load. With the output loaded to drive 2.5 ohms the voltage was 50 volts DC; this means the output current was 20 A and the power was 1 kW. The current consumed by the (220v) driving motor jumped from a typical 5-6 amps in the unfiltered state to 23 amps in the resonant state. This was far beyond the capability of the driving motor and greatly limited the amount of experimentation that could be done.

The resonant output was extremely large based on the small amount of field stimulation available from the residual magnetism. An attempt was made investigate using a demagnetizing current to reduce the effect of the residual magnetism in the resonant condition. It was hypothesized that it might be easier to modulate a resonant system with a small demagnetizing current rather than forcing a large magnetizing current into a non-resonant system. This did not work. The demagnetizing current did not linearly change the resonant output. Small demagnetizing currents had no measurable effect. At a certain threshold the character of the resonant output changed from the hex phase rectification back to the three phase rectification, and this gave a step reduction in output. The combination of the non-linear control of the resonant output and the large shaft power consumed by the condition eliminated further consideration of using this resonant state for use with generating 60 Hz power.

The resonant output was clearly caused by a combination of the capacitors filtering the phase coils and the operational speed of the alternator. One of the desired features of a high frequency alternator for producing 60 Hz power is independence from engine speed. The use of the armature filter capacitors creates undesirable resonant conditions at certain speeds. Therefore the use of filter capacitors, shown in Figure 7, is not appropriate.

3.3 Development of Modulation Despite the high inductance of the field coil the control circuit showed the ability to achieve limited amounts of 60 Hz modulation of the alternator output voltage, coupled with a substantial DC offset from zero. It was clear that the field coil inductance was too high for meaningful 60 Hz modulation.

Because of unusual the design of the truck stlye alternator, the field coil was available for rewinding; it was a stationary element. The initial field coil was 1050 turns. This was removed and replaced with 9 segments of coil, each having 140 turns of wire. The ends of each of these segments were brought out of the alternator so they could be combined in series or parallel as desired. This allowed a variation of the inductance by a factor of 81, since inductance is proportionate to the number of turns squared. Meanwhile, reducing the number of turns requires increasing the current, in inverse proportion, to maintain the same electro-motive force MMF (amp turns). For example, halving the

number of turns reduces the inductance by a factor of four, but doubles the current required for a given level of magnetization.

When the revised coils were used in the control system of Figure 5 the system would oscillate at about 20-30 Hz. Investigation of the control circuit dynamics soon made it apparent that the model for the alternator itself was deficient. It was decided to investigate the alternator performance independent of the control loop.

The initial control circuit and modulation scheme anticipated a single sided drive. The residual magnetism of the alternator introduced the need for reverse currents in the field coil. A scheme of using one of the field coil segments in reverse for "demagnetization" was considered. The difficulty of high speed modulation of the coil due to the high inductance also dictated against single sided excitation of the field coil. The envisioned rectification wave has a DC component, which is not a problem, plus a fundamental component, which is a problem due to the inductance of the field coil, plus substantial higher harmonics, which become a tremendous problem due to the inductance. It became clear that a bipolar drive using a 60 Hz AC field current was desirable since no higher harmonics would be required.

A second advantage of a AC drive for the field current was the possibility of using a tuned 60 Hz resonant tank circuit to provide high driving voltages excited by a low voltage control circuit. This approach has the advantage that the magnetic energy needed in the field during a portion each cycle is not lost upon removal, but is temporarily stored in the capacitor as electrostatic potential. Such a system was tried using the single sided drive and a transformer to block the DC and couple the AC between the control circuit and the tank circuit. See Figure 8. This did not work well, primarily because the resonant system had a low Q, quality factor, which means it had large losses. Another flaw with the system as shown is the fact that all the switching noise from the pulse width modulator (PWM) shows up directly in the tank circuit. The low Q of the system is a function of the alternator itself and not a fault of the drive system. With some current smoothing in the drive, this configuration may have potential for future alternator field control circuits.

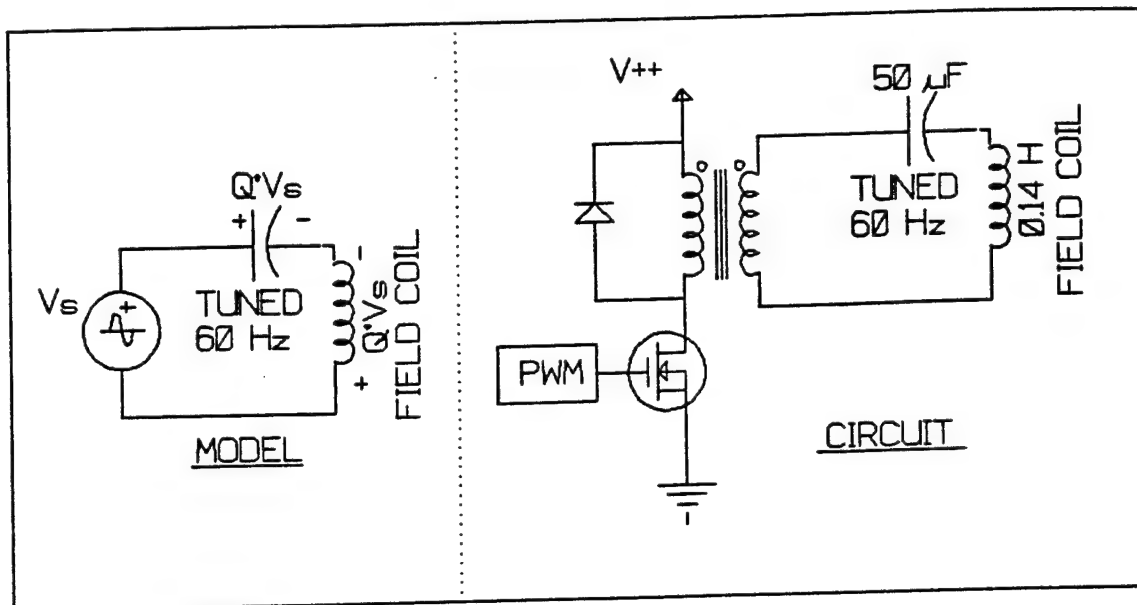


FIGURE 8

Resonant Drive with Transformer Coupling

In order to better characterize the alternator model, it was decided to go to "open loop" control. The driver was now simply line voltage (60 Hz, 120VAC) controlled by a current limiting resistor in series with the field coil. The output voltage was controlled by adjusting the current limiting resistor as shown in Figure 9.

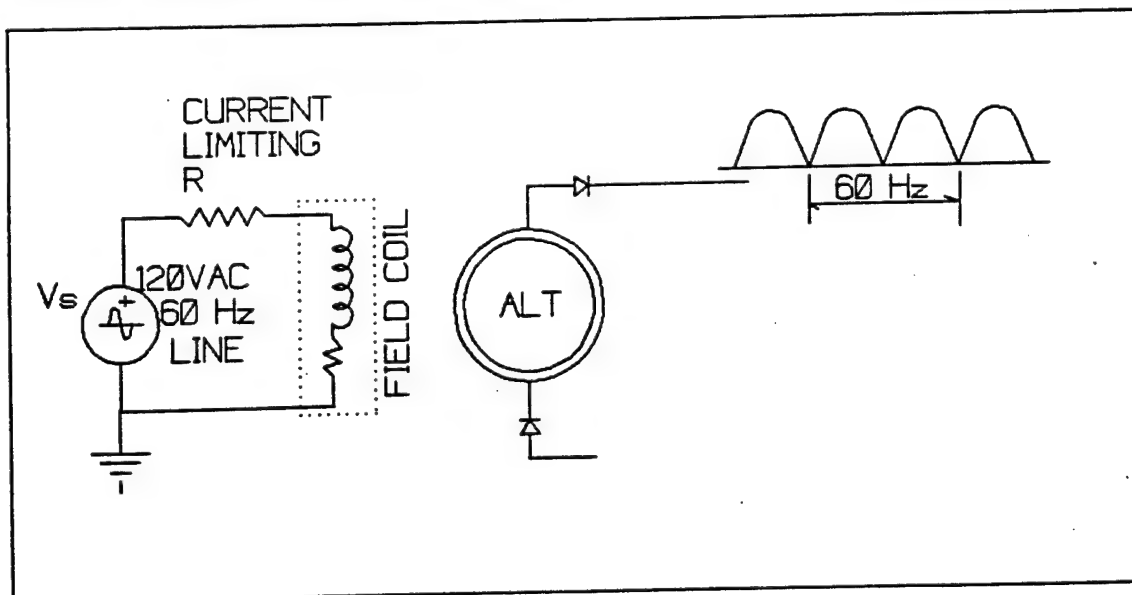


FIGURE 9

Open Loop Circuit for 60 Hz Modulation

Tests with the open loop field drive produced the desired 60 Hz rectified output ( with a DC offset due to residual magnetism ) . This also revealed the nature of the field coil/alternator model and the reason for the low Q in the resonant drive system. Figure 10 shows a typical waveform pair for field coil voltage and current. There is an unexpectedly low phase angle between the voltage and current curves. (Phase angle was estimated by averaging the delay of the zero intercepts of the current wave from the zero intercepts of the voltage waveform.) This low phase angle, usually about 40 degrees, indicates the absorption of a great deal active power. The expected phase angle would have been near to 90 degrees.

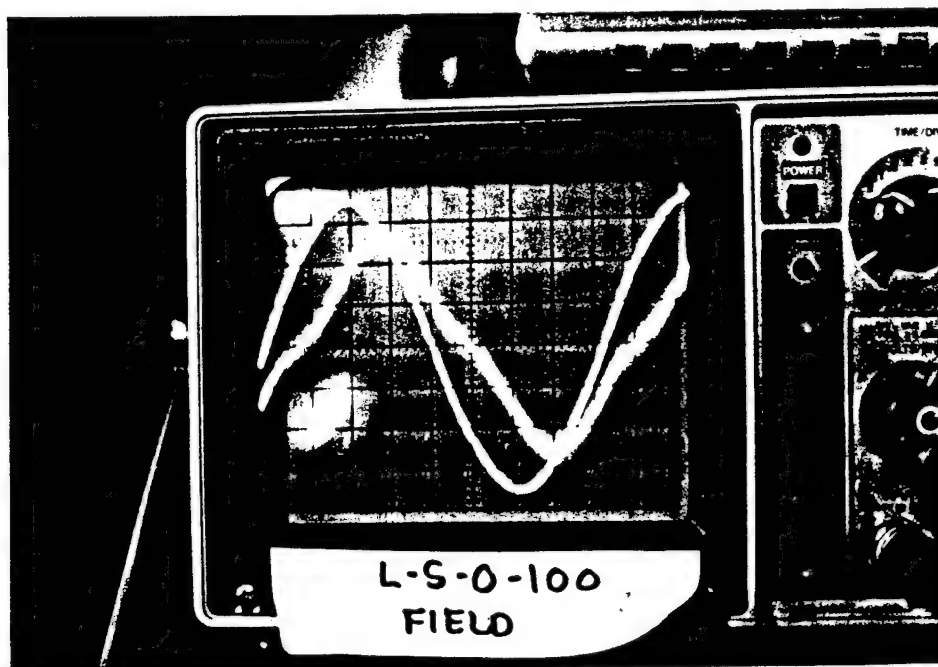


FIGURE 10

Field Coil Excitation Waveforms, Voltage Leads Current

Transformer models show a parasitic admittance in parallel with the coil to account for the energy losses and the reduced magnetic flux caused by hysteresis and eddy current losses (core losses) in the real transformer. This model matches the observed performance of the alternator. In this case the parasitic admittance absorbs a great deal of power and greatly reduces the output of the alternator. These core losses are presumed to be due to the large amounts of non-laminated steel and iron in the magnetic path of the truck style alternator. These non-laminated portions are appropriate for DC operation. For 60 Hz modulation, the core losses associated with modulating the magnetic

field in a solid iron core are excessive and make it impractical for generating AC power.

At this point in the project Gauss Corporation loaned the use of a competitor's automotive style\*\* alternator in which more of the magnetic path was made of laminated electrical steel. Interestingly, this unit showed almost identical core losses and phase angle between the field excitation voltage and current. It was also interesting that the phase angle (and core losses) remained the same for all combinations of filed coil windings on the truck style alternator. The phase angle and magnitude changed only very slightly as the load on the alternators was varied from 100 ohm to 1 ohm.

Importantly, the magnitude and phase angle of the field excitation voltage and current did not change as the motor speed was changed from 3200 RPM to 0 RPM. This indicated that the field sees only the core losses from the 60 Hz excitation and not the more extensive losses from the high frequency shifts of the magnetic field within the phases. By inference, the energy to make up for high frequency core losses must come from the shaft.

A series of 60 Hz modulation tests were performed on each of the alternator configurations with various loads. The test set up of Figure 9 was used. The field excitation waveforms were photographed and measured, including phase angle. The output voltage waveform was also measured and photographed. For the truck style alternator a filter was used on the alternator output to reduce the influence of the ripple on the measurements.

The automotive style alternator had the expected hex phase sinusoidal ripple and was therefore more suited to continued experimentation than the truck style alternator. All commutation experiments were done with this automotive style alternator.

3.4 Development of Commutation Along with modulation of the alternator output, commutation of the load relative to the alternator is a crucial element of the scheme. In general, it is not a particularly novel technique. It is used in inverter technology for much the same effect. Unlike inverters, however, in this application the high side silicon switches of an H bridge have a floating high ripple reference. A typical H-bridge arrangement was developed to handle this commutation, and an unusual photovoltaic floating trigger circuit was developed to handle the high side switching. Finally, preliminary investigations were made of an potentially more efficient alternative commutation scheme that might eliminate the H-bridge and its silicon losses.

Details of the power and commutation control circuits are shown in Appendix A. Highlights are noted in the discussions below.

---

\*\* Note: The automotive style alternator had a claw tooth shaped rotor core made of solid, not laminated, magnetic material. It is referred to in this report as the "automotive style" alternator.

3.4.1 Demonstrated Commutation Commutation was achieved by use of a H-bridge with actively controlled MOSFET switched. IRFP044 MOSFETs were chosen because of their availability and for the ease of designing drive circuitry for MOSFETs. In particular, it was desired to have a device with easy forced commutation. The MOSFET ratings were sufficient for the voltage current and power ratings proposed for this first stage development project. For full scale power IGBT devices have better ratings.

Figure 11 shows the H-bridge commutation circuit, and the schematic voltage waveforms in the circuit. Waveform (g) in Figure 11 shows the typical turn on and turn off waveforms. These rates are controlled by the resistances in the charging and discharging paths for each MOSFET. The rates have been selected to insure that all devices are off before any any pairs start conducting. This helps prevent short circuit conditions between the positive rail and ground. The turn off waveforms were 6 usec and steep, the turn on waveforms were 7 usec (microseconds) and slow to moderate in slope. This gives a period of 1 usec where all devices are off. This short period should be compared to 8300 usec conduction period for half a 60Hz sine wave. Switching is done when the alternator output voltage is modulated to zero volts, making for soft switching.

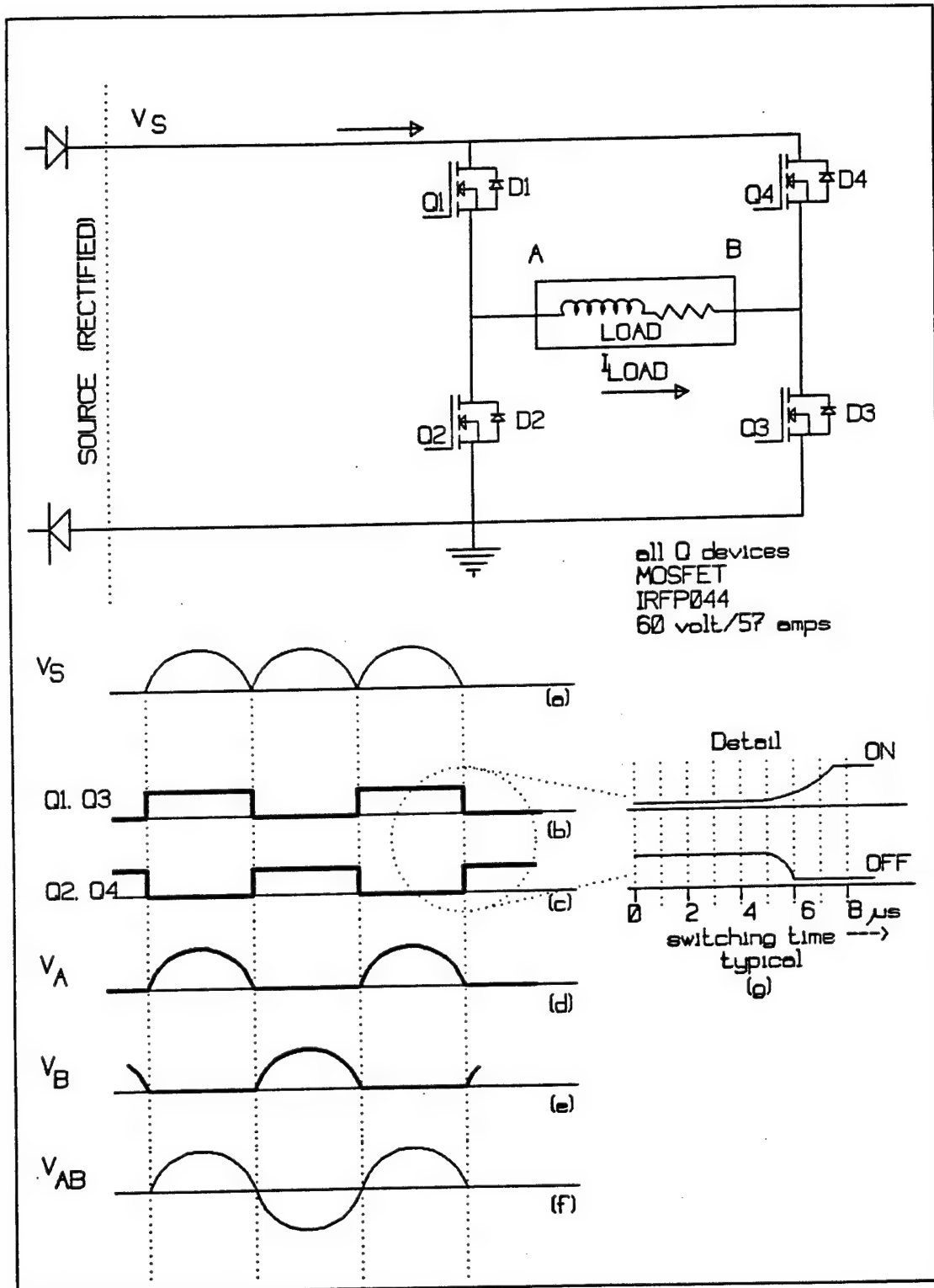


FIGURE 11

Commutation Circuit and Schematic Waveforms



Each MOSFET has a built in free wheeling diode as shown. If a reactive load still tries to drive current even though the source voltage is zero, the free wheel diodes provide connections between the ground and power rails.

The low side switches (Q2 and Q3), being ground referenced, were driven by CMOS logic. The high side switches have a floating reference. A relatively simple and rugged floating high side driver was developed using a photovoltaic source and opto-coupling transistor switches. This is shown in Figure 12. It is the opto-coupling transistors of this circuit which set the relatively slow turn on and turn off speed for the commutation circuit. The photovoltaic sources are a new product (PVI5050) from International Rectifier and work well.

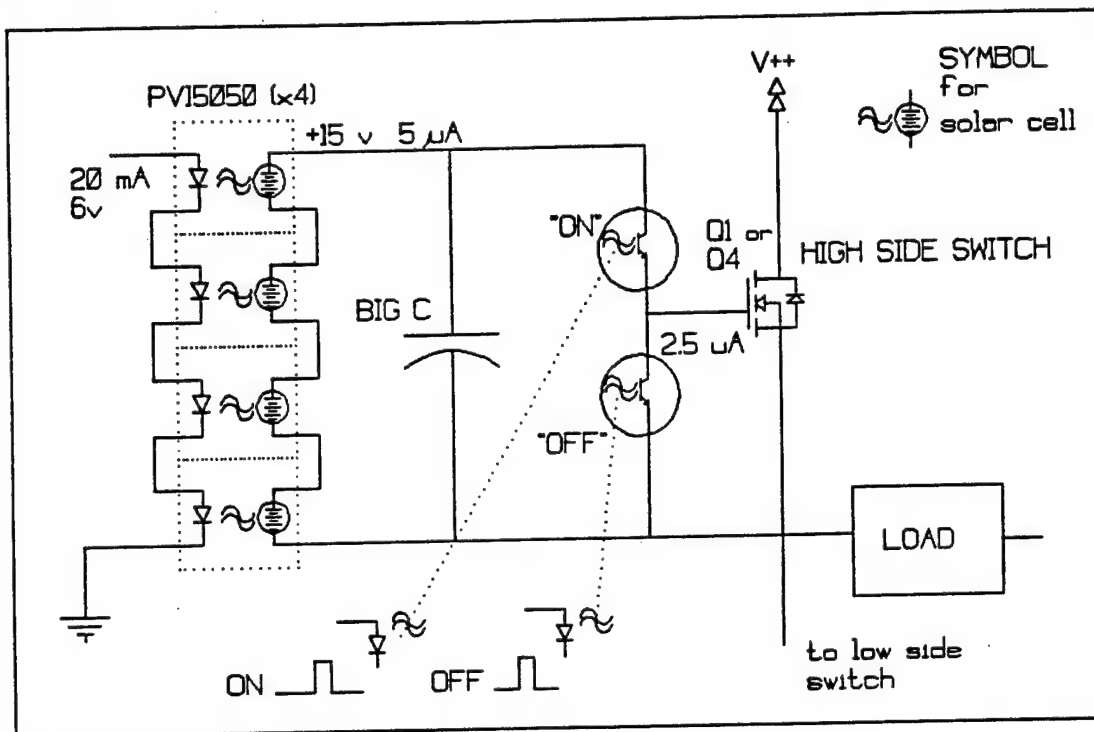


FIGURE 12

Schematic of High Side Switch

Originally the switching logic was controlled by the alternator output voltage, with switching (commutation) taking place as the output voltage neared zero. This worked for resistive loads, but reactive loads did not let the output voltage fall to zero. For example a capacitor averaged the DC content of the rectified source and did not let the supply rail modulate to zero, thus no switching occurred. This was addressed by designing the commutation trigger to sense the maximum and minimum of the reference signal, rather than the actual output.

Due to the field coil's inductance, the field current and the modulated output cross zero 90° behind the field driving voltage. The commutation

trigger circuit obtained this by differentiating the reference signal. This worked fine with resistive loads, and with reactive loads driven by a rectified line source or by the alternator. However, differentiation magnifies noise. An integration approach, instead of differentiation, might minimize this noise and lead to a more robust system.

Tests were performed with the commutation circuit coupling various resistive loads (75 ohms to 1 ohm) with the 60 Hz modulated output of the automotive style alternator.

**3.4.2 Alternative Commutation Method** Preliminary investigations were made into an alternative system of commutation. By replacing the normal six rectification diodes (Shown back in Figure 1) with 12 SCRs, as shown in Figure 13 it would be possible to completely eliminate the B bridge circuit and all of its silicon resistive losses. The SCR gates A and B are shown along with the rectified output voltage  $V_{xy}$ . Note that in this arrangement one end of the load is always grounded, which is more traditional than the commutated ground shown in Figure 11.

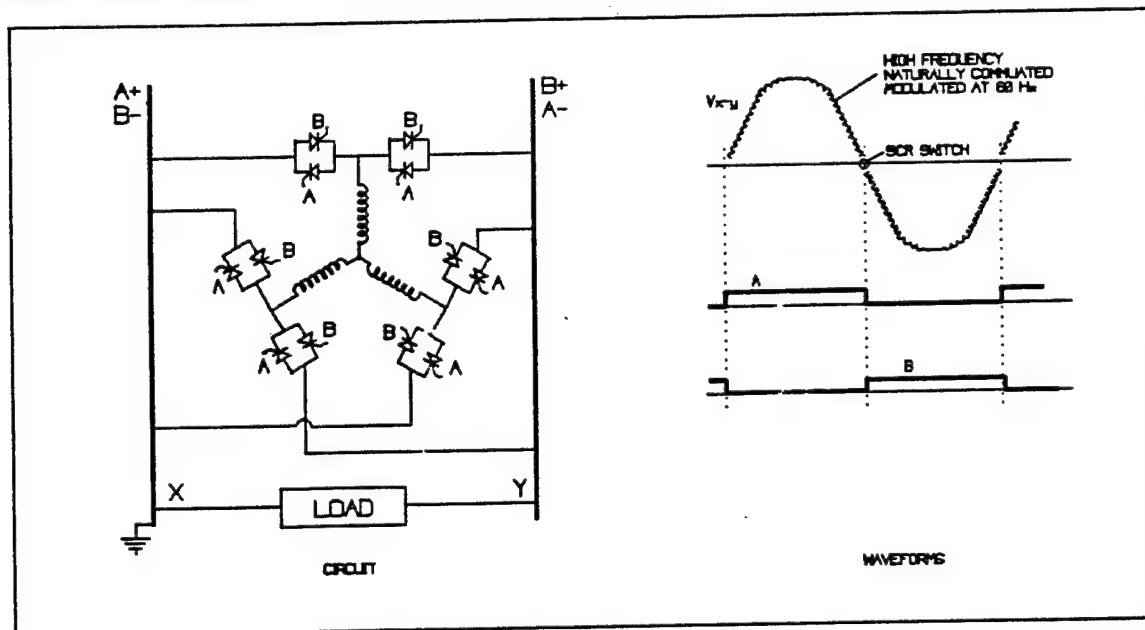


**FIGURE 13**

Alternate Commutation Scheme with Twelve SCRs

SCRs are more rugged than MOSFETs. At any one time only two SCRs are used in series, just as with the six diodes. Like diodes and IGBTs, SCRs have a fixed voltage drop regardless of current level, which makes them attractive in terms of power loss at high currents. There are no other silicon drops in this circuit, so commutation comes at no additional losses beyond those inherent in the rectified output of all high frequency alternators.

The circuit of Figure 13 proposes an unusual operating condition for SCRs. The gating signals A and B will be on for the complete half cycle of the 60 Hz modulation. Meanwhile, the SCR will see approximately 500-800 Hz high frequency alternator output and will be asked to perform natural commutation with the other activated SCRs and to provide reverse voltage blocking while gated on. (Normally, SCRs are triggered on and then the gate is removed. Natural gain of the device keeps it triggered until the current drops to zero.) Reference 1<sup>\*\*\*</sup> cautions that for dynamic gate SCRs "allowing a positive gate while the SCR becomes reverse biased limits device reliability" (p22-45).

Preliminary tests used the circuit of Figure 14. The SCR worked but allowed a small reverse current through the load when the gate was "on" and the SCR was reverse biased. This current was controlled by the voltage and resistance of the gate circuit, but was independent of the reverse bias voltage. The mechanism (path) for this reverse current is not known. This current was not influenced by the magnitude of the reverse voltage blocked by the SCR. The influence of this small reverse current on the proposed commutation scheme is not yet certain. It was not possible to investigate three phase commutation of this scheme due to limitations of the hardware.

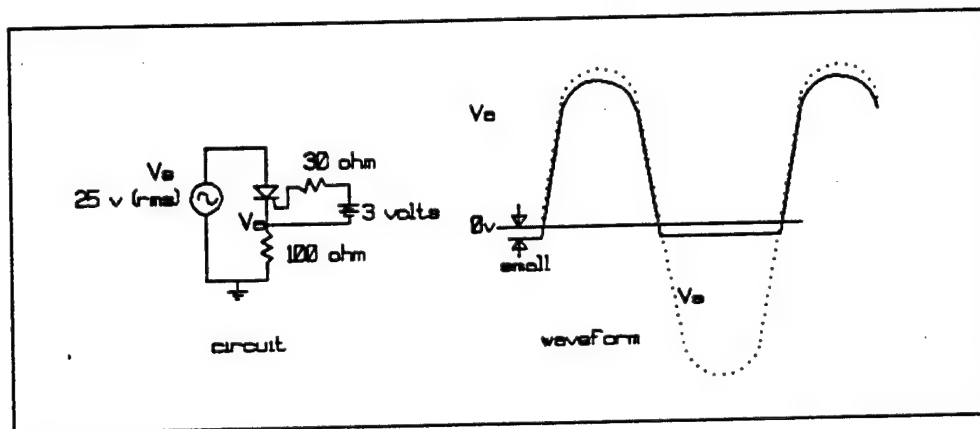


FIGURE 14

Test Set Up for Gated SCR Commutation Trials (single phase.)

**3.5 Demonstration of Reaction Current Handling** Since the alternator source is a rectified source it can not accept reverse current flow. This is fine for resistive loads, but reactive loads store energy during part of each cycle and then try to return that energy to the source in another portion of the cycle. In effect, the reactive loads see a low impedance source when they draw energy and an infinite impedance source when they need to return energy. This causes non sinusoidal waveforms.

A reactive branch was added in parallel with the load and was controlled to have an impedance to complement that of the source. That is, the

\*\*\* Reference 1: Fink and Beaty, "Standard Handbook for Electrical Engineers", 12th Ed., 1987, McGraw Hill, NY.

reaction branch impedance was high when the source was low and low when the source was high. This allowed the load to see a low impedance at all times. The reaction branch is shown in Figure 15. It consisted of a shunting resistor gated to ground by a MOSFET, which in turn was controlled by a sensing circuit. The sensing circuit opened the MOSFET and the reaction branch whenever the load was trying to drive the source; it turned off the reaction branch whenever the source was driving the load.

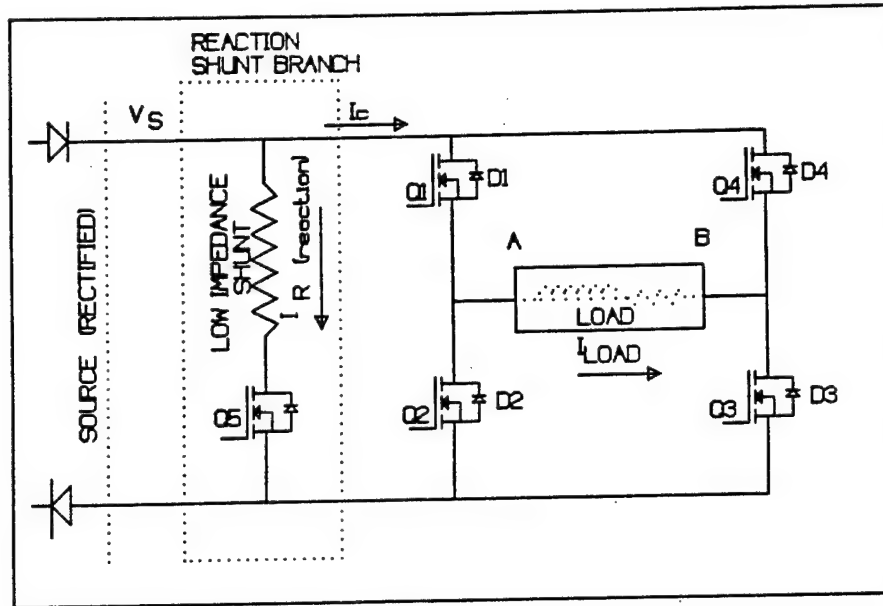


FIGURE 15

Reaction Branch Circuit

Originally the reaction branch trigger tried to sense when there was current through the free wheel diodes in  $Q_2$  and  $Q_3$  of the commutation circuit. This was not successful since the gated (on) MOSFETs could support quite a large reverse current that bypassed the diodes. As a temporary measure an additional sense diode was placed in the source line in order to isolate the source and the load voltages. A pull down resistor was used with the source voltage. The trigger circuit sensed the source and load voltages across the sense diode and opened the reaction branch whenever the load tried to drive the source.

As the reaction branch triggered oscillations were sometimes a problem. Additional switching hysteresis (not magnetic) was added to the comparators and an inductive coil with free wheeling diode was added to the reaction branch. This coil prevented instantaneous changes in the reaction current and allowed for a graceful transition from high impedance to low. The modified reaction branch with sense diode, inductive coil and free wheel diode are shown in Figure 16. Details of the control circuit are shown in Appendix A.

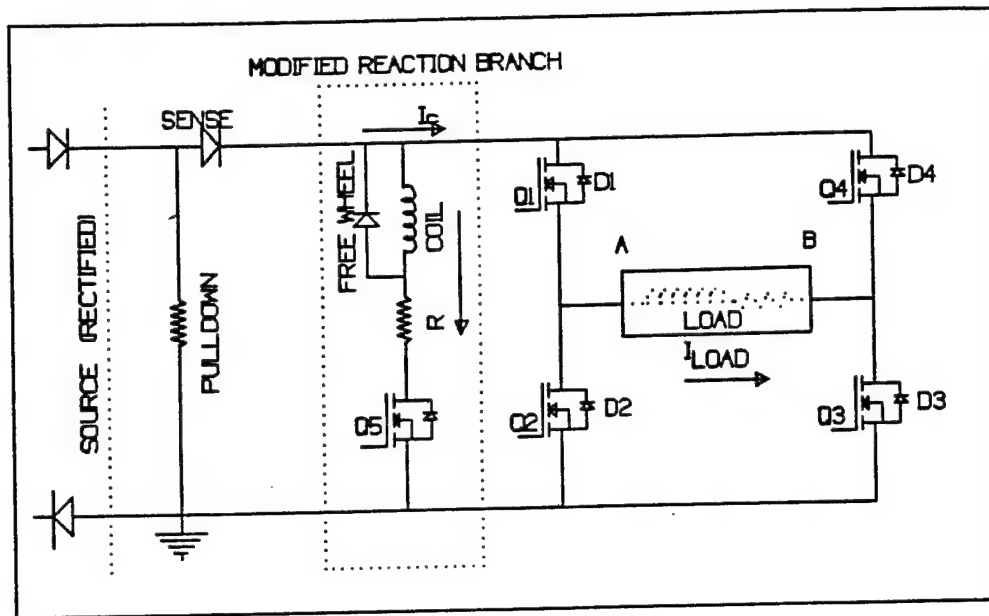


FIGURE 16

Modified Reaction Branch with Sense Diode, Coil, and Free Wheel Diode

The reaction branch was tested by switching in capacitive and inductive series loads. This was tested with both a rectified line source (transformed to 25 volts RMS) and the automotive style alternator source modulated and commutated at 60 Hz.

3.6 Analytical Development Two major questions based on the development project were:

Could the high frequency alternators be designed to minimize the effect of hysteresis and eddy currents on the field? and,

Could the high frequency alternators be scaled up to produce 120 VAC power?

These questions were addressed by the the preliminary sketch design of an idealized alternator with a magnetic path made entirely of laminated electrical. This alternator had a target rating of 120 V rms and 50 A rms for a output of 6 kW. Details of this calculation are shown in Appendix B.

The alternator was assumed to run at a nominal shaft speed of 6000 RPM. It was patterned after the Electrodyne heavy duty brushless alternator, with fixed field and armature coils. It had three phases separated by 120° and was designed to produce hex phase commutation patterns as shown back in Figure 1. Each phase was broken into 4 pole segments for a total of 12 poles. The field coil and and armature coil segment configurations are shown in Figure 17. The three phases were excited in

parallel. For each phase the high frequency alternations of flux were assumed to vary sinusoidally with rotor position. For ease of description and calculation this was accomplished by the varying the area of the air gap due to rotor overlap. The rotor is assumed to have 8 sinusoidal variations of overlap with each revolution. This leads to a fundamental frequency of 800 Hz for each phase, and 4800 Hz for the hex phase rectification. The total area of the three phases does not vary with rotor position, which allows the assumption of constant total flux and MMF.

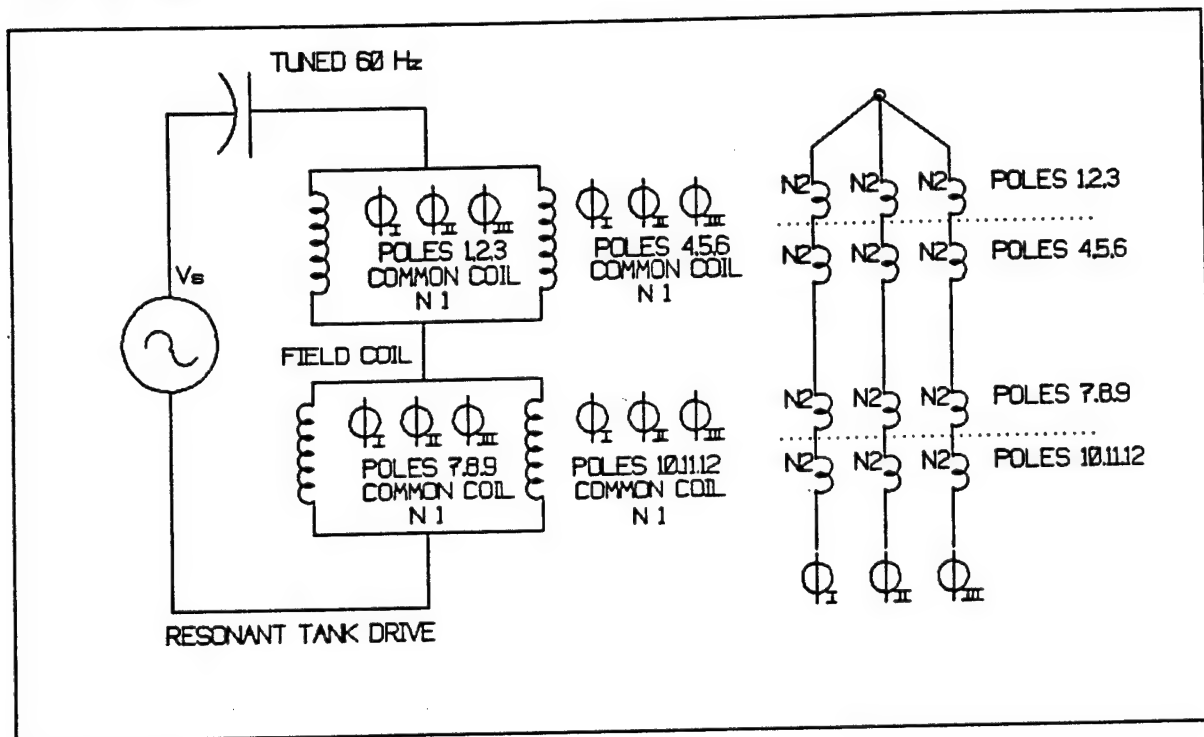


FIGURE 17

Schematic of Field and Armature Coil Arrangement in Sketch Design

The poles are arranged so that the changes in MMF due to load current offset each other as the pole voltages are added in series. This helps minimize the influence of load current on the field and on the output voltage. However, to minimize the required field currents, the allowable variation of MMF within a pole, due to load current, was set at  $\pm 50\%$  of nominal. This is a high level of fluctuation, and has a large impact on the maximum flux density and thus core losses. Greater field current compared to output current minimizes the variation of MMF from nominal, and reduces the peak flux density. This in turn minimizes the core losses, which vary as the peak flux density squared.

For first approximations all reluctance is assumed to be in the air gap, not in the magnetic material. There are assumed to be no stray inductances.

The magnetic path was assumed to be made entirely of 30H083 grain oriented Epstein annealed parallel grain electrical steel. Figure 18 shows a sketch of the proposed laminated magnetic path for a single pole. (In this sketch the reluctance is modulated, as the rotor turns, by variation of the air gap length instead of area.) Data published in Reference 1 (p 4-104) have been replotted and the core losses are estimated at  $17 (B_{\text{max}}-800)^2$  watts/lb at 800 Hz and  $0.31 (B_{\text{max}}-60)^2$  watts/lb at 60 Hz. It was further assumed that the grain orientation is optimum at all places in the magnetic path.

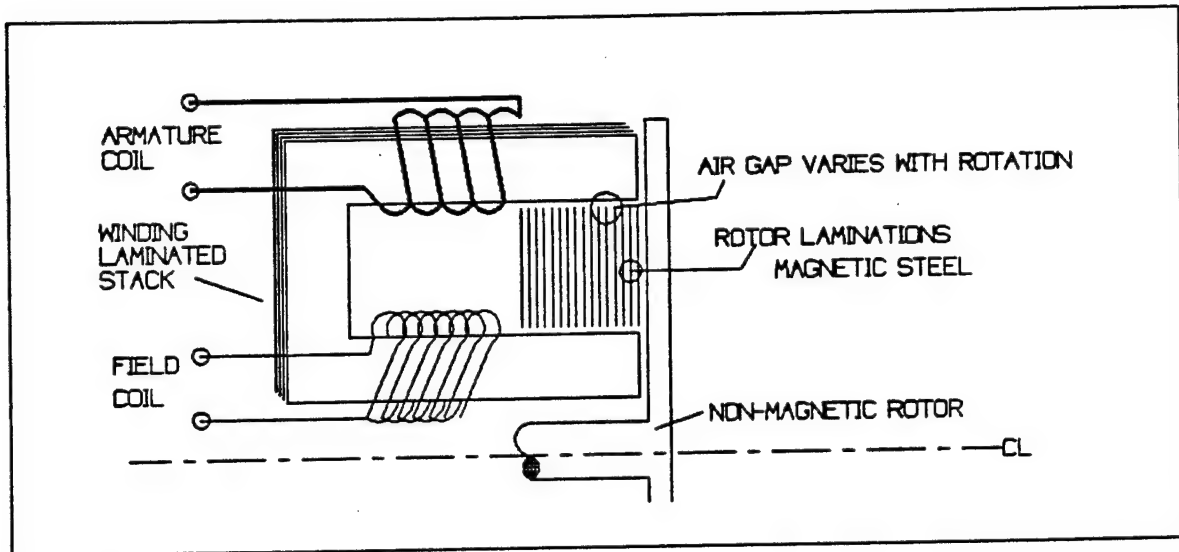


FIGURE 18

Magnetic Path Entirely of Laminated Steel for Sketch Design

A crucial assumption in this analysis is that induction values ( $B_{\text{max}}$ ) given in Reference 1 refer to the amplitude of induction modulation at the given frequency (i.e. half the peak to peak value) and that this can be applied without regard to the average level of induction provided that the total induction does not exceed saturation levels. This is important since the mechanics of the alternator depend upon the variation of the magnetic field around an average value that is not zero.

A second assumption in this analysis is that the core losses at different frequencies can be treated independently. As discussed above, the 60 Hz field excitation losses can be demonstrated to be independent of rotor speed and thus independent of the high frequency core losses. An explanation of the core loss calculation can be found in Appendix C.

The field was to be driven by a 60 Hz modulation. As shown in Figure 17, it was assumed that the field could be driven by a resonant tank circuit drive with a High Q so that coil voltage could reach 440 V RMS. This was then checked based on the core losses from modulating the

field. To minimize core losses, the nominal flux density was limited to 1.87 Tesla, which impacted directly on the required cross sectional area of the magnetic path and thus the weight.

The sketch design calculations established the following physical parameters for the idealized alternator:

constraints set:

$V_t$  - Field coil resonant drive voltage (set at 440V)  
 $B_{max}$  - maximum flux density (set at 1.87 T)  
 $\Delta$  - change in MMF due to load current in a pole (set at 0.5)  
 $N_2$  - number of armature coil turns per pole (set at 5 turns)

established by calculations:

$N_1$  - number of field coil turns  
 $I_t$  - Field coil current (total)  
 $L_t$  - Field coil inductance (total)  
 $g$  - air gap length  
 $A_{nom}$  - magnetic path nominal cross section area, each pole  
 $P_{60}$  - Core\* losses (watts/lb) from 60 Hz Modulation of Coil  
 $P_{800}$  - Core\* losses (watts/lb) 800 Hz alternations  
(\* hysteresis and eddy current losses combined)

From these parameters the physical dimensions of the magnetic path were laid out leading to an estimated weight of magnetic material (minimum) and then the actual losses. From these losses the equivalent field coil core loss admittance was calculated, and the  $V_s$  - Field circuit driving voltage was determined along with the  $Q$  for the resonant circuit.

It is certain that a practical machine would not be as attractive as this idealized machine. The primary differences would be the effect of stray inductances and additional metal required for a the magnetic path.



#### 4. DISCUSSION OF RESULTS

4.1 Overview and General Results Using the automotive style alternator, the project demonstrated the production of 60 Hz AC power. The output was modulated at 60 Hz and a commutation circuit unfolded the rectified output of the alternator to provide a sine wave to the load. Figure 19 shows a photograph of the alternator's waveform when driving a 75 ohm load with a sine wave 50 volts peak to peak. A reaction circuit was built and demonstrated the use of a low impedance path for reactive loads to return stored energy so that the voltage and current waveforms in the load were the desired sinusoidal shapes.

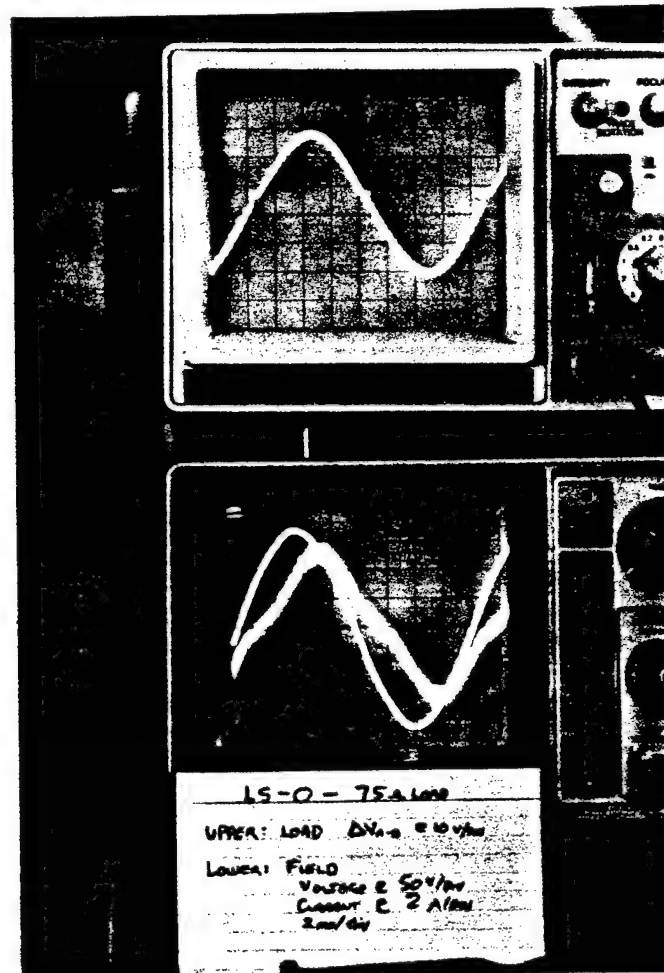


FIGURE 19

Waveforms of a high frequency alternator driving a 75 ohm load with 60 Hz AC power, 50 volts peak to peak. Upper waveform, load voltage (differential); lower waveforms field excitation, voltage leads current.

Unexpectedly, it was found that the field absorbed a great deal of active (resistive) power when modulated at 60 Hz. Independent of load or output power, the field of the automotive style alternator absorbed 307 watts of active (resistive) electrical power. This was in addition to the power supplied by the shaft, and indeed was independent of shaft

speed. For comparison, when driven by this field excitation, the alternator was able to produce a maximum of only 137 watts of 60 Hz AC power. The field losses can be inferred from the field excitation waveforms of Figure 19 in which the current (10 amps peak to peak) lags the voltage (350 volts peak to peak) by about 40 degrees. The apparent power driving the field, including energy stored in the field and then returned to the driver, is about 420 V-A.

The high losses encountered in modulating the field are explained by power absorption in hysteresis and eddy current losses in the magnetic circuit. These core losses are presumed to be excessively high in existing alternators due to the use of unlaminated steel and iron in the magnetic paths. According to Reference 1 (p 2-21) eddy current losses vary inversely as the square of the number of laminations into which a given solid core is broken. The unlaminated materials are appropriate for use in generating "DC" because the fields are not modulated. For the proposed method of producing AC power modulation is important. The excessive field losses make the scheme impractical using existing alternators.

The analytical development step produced a sketch design of an alternator with a magnetic path made of all laminated materials in order to confirm the possibility of scaling the alternator output to 120 VAC at 6 kW. In this sketch design the field core losses due to 60 Hz modulation were reduced to 22 watts for 6 kW of alternator output.

Along each step of the development procedure there were specific results that lent insight to the overall result. These are summarized in the sections below.

4.2 Results of Tight Regulation Development The development of the tight regulation control brought a number of issues to light. These issues included the difficulty of using a single sided control, the high inductance of the truck style alternator field coil, the unusual ripple output of the truck style alternator, attempts to filter the ripple output of the truck style alternator, the magnetization curves of the alternators, and the drop of output voltage with load. Finally, open loop control was used. First this was done to develop a better understanding of the alternator performance independent of the control loop. Because of using open loop control the high core losses were discovered in the field circuit. It became apparent that closed loop control was not warranted at this stage. Thereafter demonstrations of the 60 Hz modulation and commutation were done with open loop control.

Figure 20 shows a typical magnetization curve for the truck style alternator. The effects of hysteresis and residual magnetism are clearly evident. This curve was obtained by exciting the alternator field with a quasi-static current and measuring the steady state output. The exciting current was increase in steps to the maximum and then decreased in steps to zero in order to show the hysteresis.

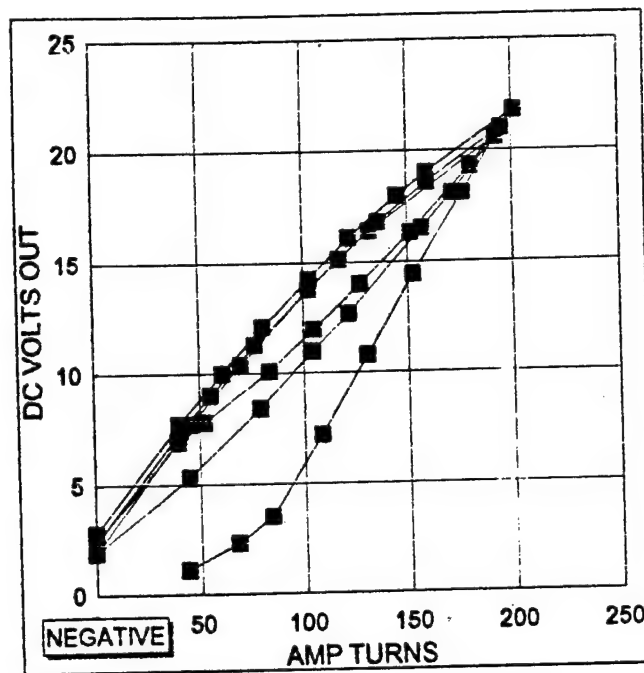


**FIGURE 20**

Typical Alternator Magnetization Curve Showing Hysteresis and Residual Magnetism (Truck Style Alternator, Field Coil 280 Turns)

**4.2.1 Single Sided Control.** The original scheme called for replacing the normal single sided voltage regulator of the alternators with a similar design that could follow a moving reference. This worked only for slowly varying signals which did not require the output to go below the output voltage produced by residual magnetism. (This was an output of 1-5 volts depending on load and previous magnetization.) The original design concept envisioned a single sided control following a rectified sine wave reference and modulating the output in like manner. The inability of a single sided control to bring the output below the residual magnetism level made use of the single sided control impractical. Also, the need for high frequency components of the fundamental when following a rectified sine made use of the single sided control impractical.

Some type of bipolar drive for the field coil was indicated. Two were tried. First a transformer coupling of the single sided driver to the field coil through a resonant drive circuit was tried. This worked poorly because of the low Q, quality, of resonant loop. This low Q was probably due to the high core losses in the magnetic circuit. Also all the switching noise from the pulse width modulation of the single sided driver showed up in the coil drive loop. The second bipolar drive simply placed the field coil in series with a current limiting resistor and line voltage. This open loop "control" worked well and formed the basis for subsequent investigations

#### 4.2.2 High Inductance of the field coil (truck style alternator)

The truck style alternator's field coil inductance (in place in the magnetic circuit) was measured through its response to a step voltage change. The time constant was 0.45 seconds, which indicated an inductance of about 6 Henries (H). This high inductance, efficient for DC operation, tremendously limited the amount of 60 Hz modulation of the magnetic field that could be accomplished with practical voltages. To remedy this, the coil was rewound from one 1050 turn coil to 9 segments of 140 turns each. These segments were combined in various series and parallel configurations, which allowed the inductance to be varied from 8.9 H to 0.14 H. Each time the number of series turns is cut in half the needed current is increased by a factor of two and the inductance is decreased by a factor of four. When the smaller inductance coils were placed into the single sided control loop (closed loop), the control loop, which had been able to control limited 60 Hz modulations of the high inductance coils, started to oscillate at 10-30 Hz. It was in addressing these oscillations that open loop control was tried and the high core losses of the field uncovered.

Fortunately the automotive style alternator's field coil inductance was not too high (near 0.5 H, although it was not measured directly). The field coil on the automotive style alternator was not available for rewinding. Clearly the field coil inductance is an important parameter for alternator design for use in 60 Hz modulation.

4.2.3 Ripple in the alternator output. The truck style alternator had a very large ripple of unusual character and one half the expected frequency. See Figure 6. The output ripple was large enough and its frequency (about 1200 Hz) was close enough to the desired 60 Hz modulation frequency that filtering the ripple for use in the control circuit was difficult. The attempt to filter the ripple with capacitors prior to the rectification diodes produced a smooth waveform, but introduced armature resonance reactions that were uncontrollable. See Figure 7. At the right shaft speed the unexcited alternator output grew to 249 volts DC (no load), and produced 50 volts DC when driving 2.5 ohms of load. This means it produced a power output 1 kW when stimulated only by the residual magnetism. Attempts were made to control this output by adding "demagnetization" current in the field coil. This only produced a non linear step change in the output level and a simultaneous shift in its character. When in this resonant mode the current drawn by the motor driving the alternator jumped from 6 to 23 amps. This resonant mode was speed dependent. The approach of filtering the armature voltages as shown in Figure 7 was not useful for the planned 60 Hz modulation of alternator output.

Fortunately, the automotive style alternator was available which provided the expected hex phase rectification ripple. See Figure 1. This alternator was eventually used for the modulation and commutation demonstrations.

4.3 Results of Development of Modulation Modulating the quasi-DC rectified output of the alternator was an essential part of the scheme

to provided 60 Hz AC power. A number of difficulties were encountered in modulating the output.

As described in section 4.2.2 the high inductance of the field coil of the truck style alternator did not allow for meaningful amounts of 60 Hz modulation of the magnetic field. This was successfully overcome in two different ways, first by rewinding the field coil with fewer series turns, and later by using an automotive style alternator with a lower field coil inductance.

The residual magnetism (from hysteresis) foiled the original plans to modulate the output to zero volts to follow a rectified sine wave reference. This eliminated plans to use a simple single sided field coil drive circuit. This issue was addressed by using a bipolar field drive circuit.

An attempt to couple the single sided drive into a bipolar 60 Hz resonant (tank) field coil circuit via a transformer was not successful. This was due to excessive core losses in the magnetic circuit of the field. This approach was also plagued by switching noise from the single sided driver. Later analysis showed that this approach could be made to work if a better magnetic path were used with the field coil.

Open loop control using line voltage to drive the field coil was successful. This produced modulated output as shown in Figure 21 where the automotive style alternator was modulated at 60 Hz. The rectified output is the alternator output. The high frequency ripple is visible. The ripple becomes larger and the amplitude of output modulations becomes smaller as the load current increases. This can be noted in Figure 22. In each photo the sine wave is the driving voltage to the field coil. Note the  $90^\circ$  phase shift between the driving voltage and the lagging output voltage. This held for all levels of load current. This lag was as expected since the output voltage depends on the field coil current, which should lag the field voltage by  $90^\circ$ . Note the difference in heights of each rectified "bump". This is an effect of the residual magnetism. It becomes less of a factor with increasing load and with increasing output voltage. This should also be less of a factor if laminated electrical steels were used in the magnetic path.

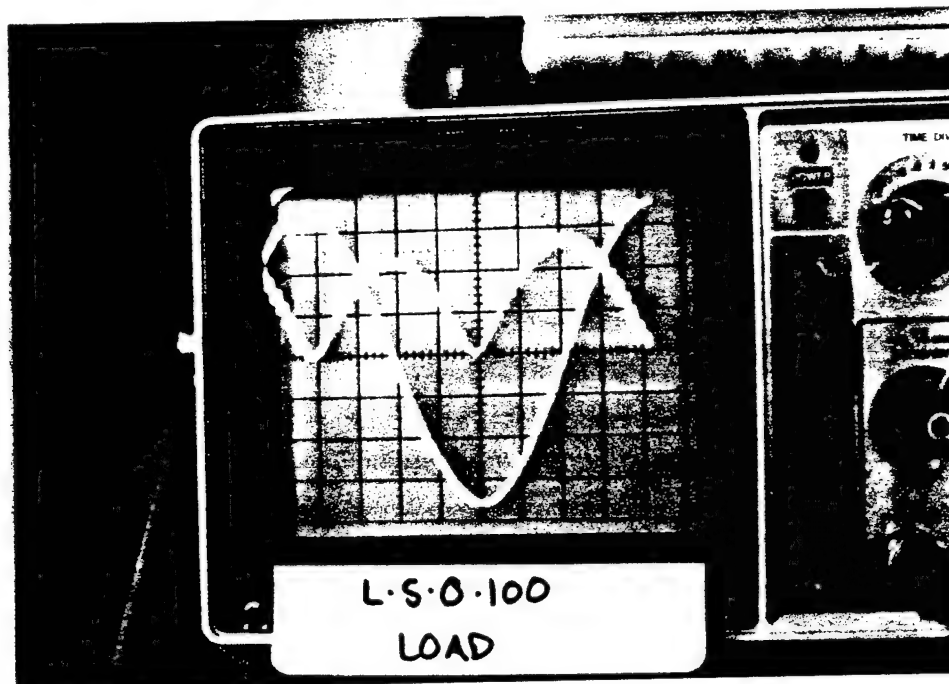


**FIGURE 21**

100 OHM LOAD: Modulated output of automotive style alternator at 60 Hz. Field driving voltage waveform at 50V/div. Rectified output voltage waveform at 10V/div. Time base is 2ms/div.

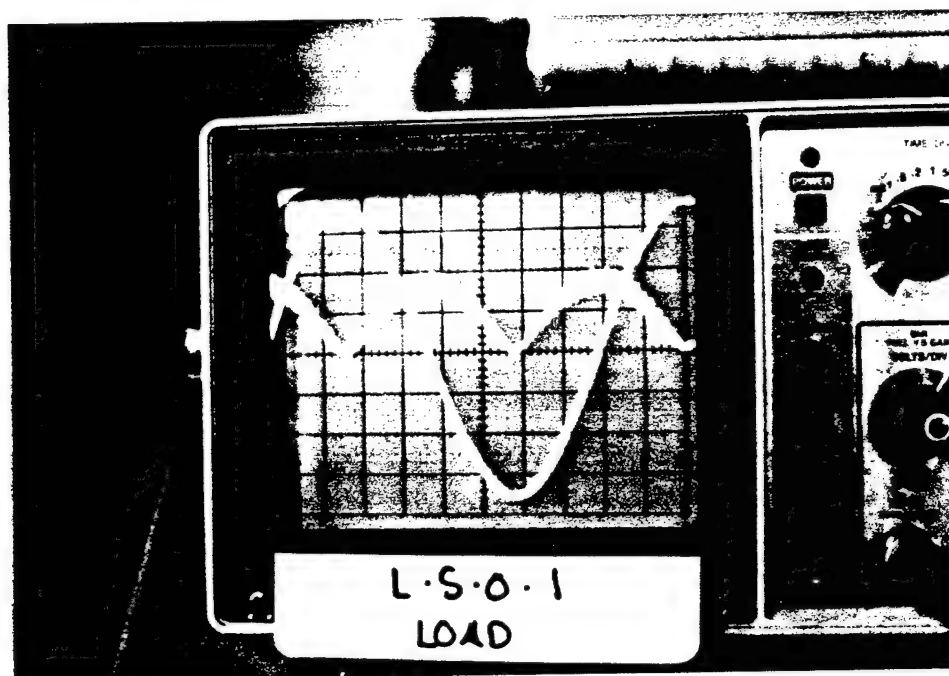


**FIGURE 22**

1 OHM LOAD: Modulated output of automotive style alternator at 60 Hz. Field driving voltage waveform at 50V/div. Rectified output voltage waveform at 10V/div. Time base is 2ms/div.

The field circuit draws excessive amounts of active power as can be seen from Figure 23. Note the phase angle between the voltage (sine wave), and the lagging current (distorted by the non linear magnetic path).

This angle ranged from  $37-43^\circ$ , increasing very slightly with increasing current. The active power is proportional to the voltage times the current times cosine of phase lag angle. The expected phase lag was near  $90^\circ$ . The observed phase lag is explained by power losses in the magnetic circuit of the field. These power losses are attributable to the hysteresis and eddy current effects (core losses) in the unlaminated portions of the alternator's magnetic circuit. Figure 23 shows the field excitation waveforms for the heavily loaded alternator driving a 1 ohm load, the output of which is shown in Figure 22.

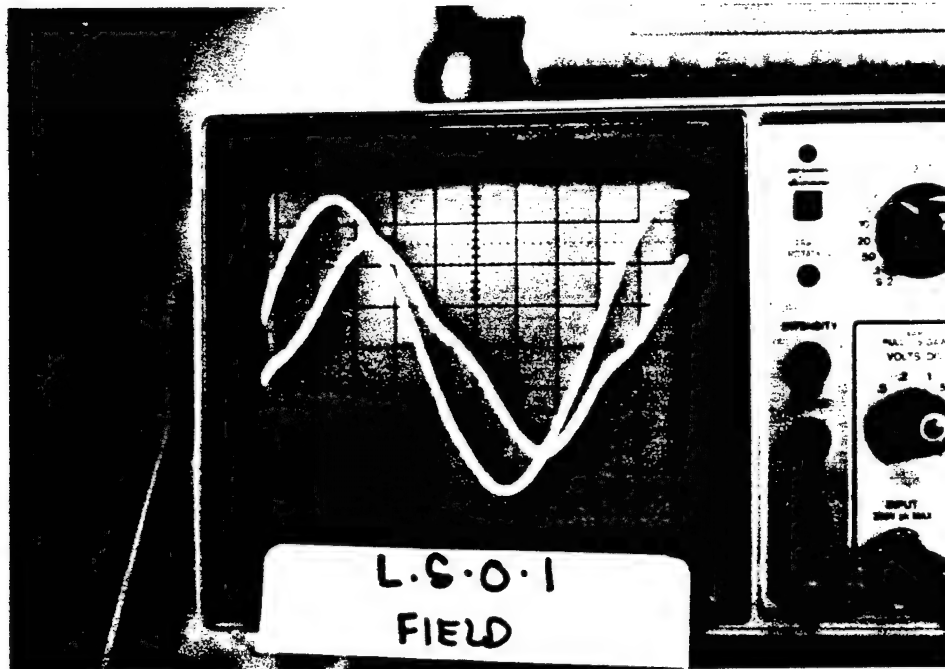


**FIGURE 23**

60 Hz field excitation waveforms for Figure 22. Alternator speed is 5382 RPM. Load is 1 ohm. Driving voltage waveform at 50V/div. Current waveform at 2 A/div. Time base is 2ms/div.

An important finding is that the field excitation power is relatively independent of both the load current and shaft RPM. This can be seen by comparing the zero RPM case of Figure 24 with high load, high RPM case of Figures 22 and 23. The field excitation curves are very similar. An important aspect of this finding is that the 60 Hz core losses seen by the field are separate from the (larger) high frequency core losses related to producing output power.

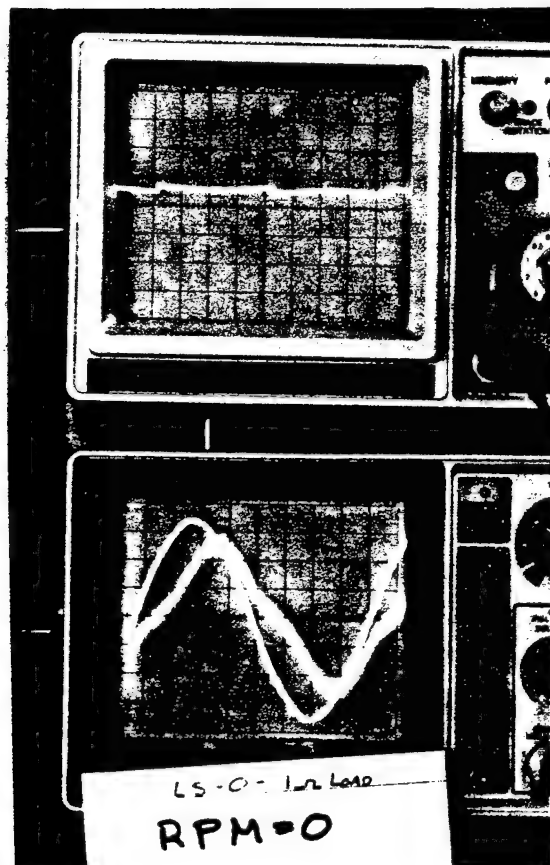


**FIGURE 24**

60 Hz field excitation waveforms for alternator at ZERO RPM. Driving voltage waveform at 50V/div. Current waveform at 2 A/div. Time base is 2ms/div.

Similar 60 Hz modulations of the truck style alternator were possible with the field coil rewound to 140 or 280 series turns. The large ripple output of this alternator made it less attractive for the formal demonstrations of modulation and commutation.

#### 4.4 Results of Development of Commutation

4.4.1 Demonstrated Commutation The commutation circuit worked in a very straight forward manner and was able to switch the output of the automotive style alternator from its rectified and modulated form, shown back in Figures 21 and 22, to the sinusoidal load voltage forms shown in Figure 25.



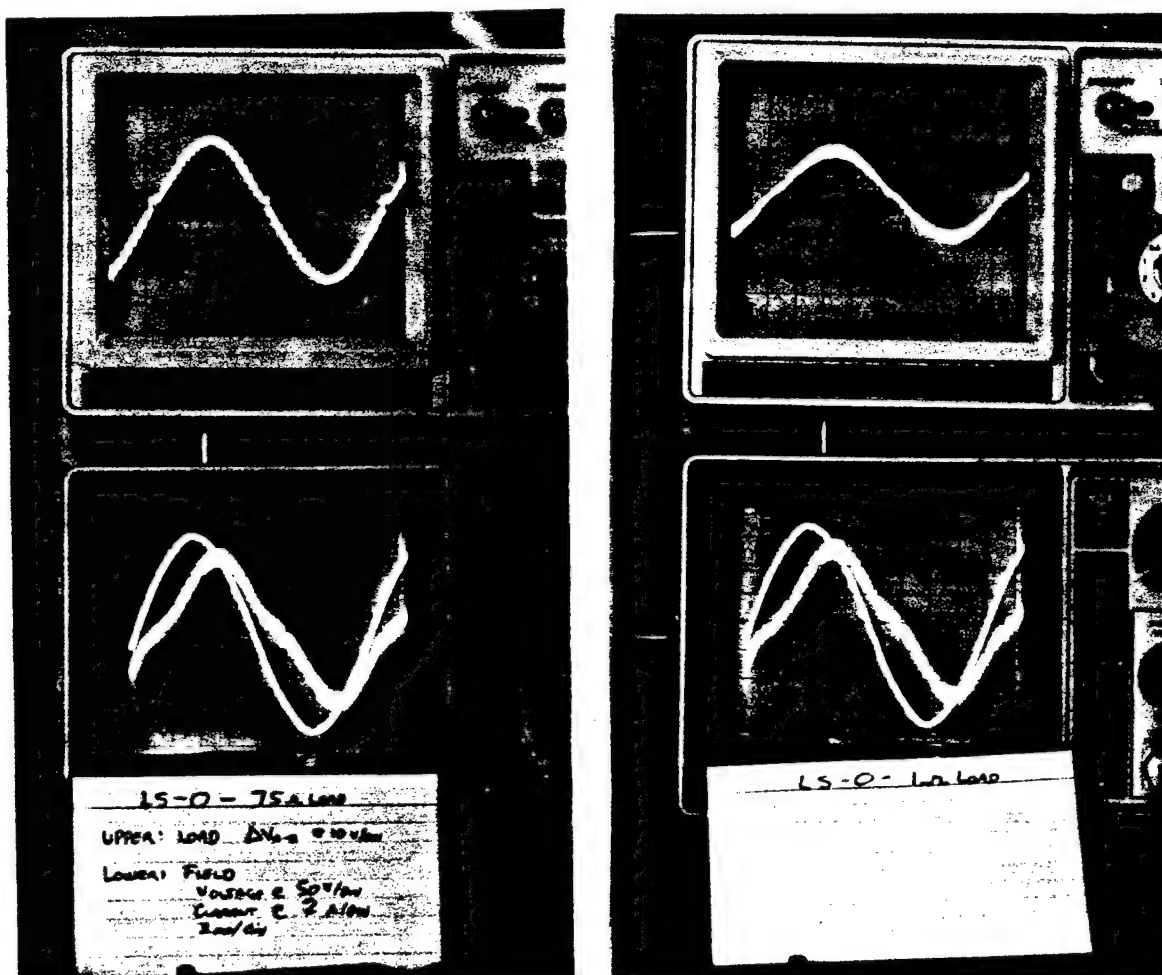


**FIGURE 25**  
**COMMUTATION**

60 Hz AC power produced by commutating the modulated output of a high frequency alternator.

Left: 75 ohm load.

Right: 1 ohm load.

Upper waveform, differential load voltage (10V/div).

Lower traces: field excitation waveforms, current lags voltage.

Current 2A/div, Voltage 50V/div, Time base 2ms/div.

4.4.2 Alternate Commutation Scheme (12 SCRs) The preliminary tests on the alternative twelve SCR commutation technique were intriguing. The SCR was able to block reverse voltages and naturally commute even when continually gated on. No problems of reliability were discerned in several hours of continuous operation. There was a problem of a small "DC" reverse current through the load as the diode was in the blocking state. This reverse current, the path for which is not understood at this time, was influenced directly by the gate driving voltage and resistance, but not by the reverse (blocked) voltage.

4.5 Results of the Development of Reactive Load Handling Since the rectified output of the alternator would not accept current flow back

from the load, the reactive loads were handled by switching in a low impedance shunt whenever the load tried to drive the source. Critical to the success of the reactive branch switching was the proper level of switching hysteresis in the trigger circuit. Also the inclusion of a inductive coil in the reaction branch helped eliminate oscillations.

The reaction branch switching is not really needed when the total load has its own low impedance shunt components. It is required, however, if one desires to maintain a sinusoidal current waveform in a reactive series circuit.

The reaction shunt branch was successful. Loads from 0.6 leading power factor to 0.1 lagging power factor were successfully and smoothly handled so that switching transients were minimal and the load currents were near sinusoidal. Samples are shown in Figure 26.

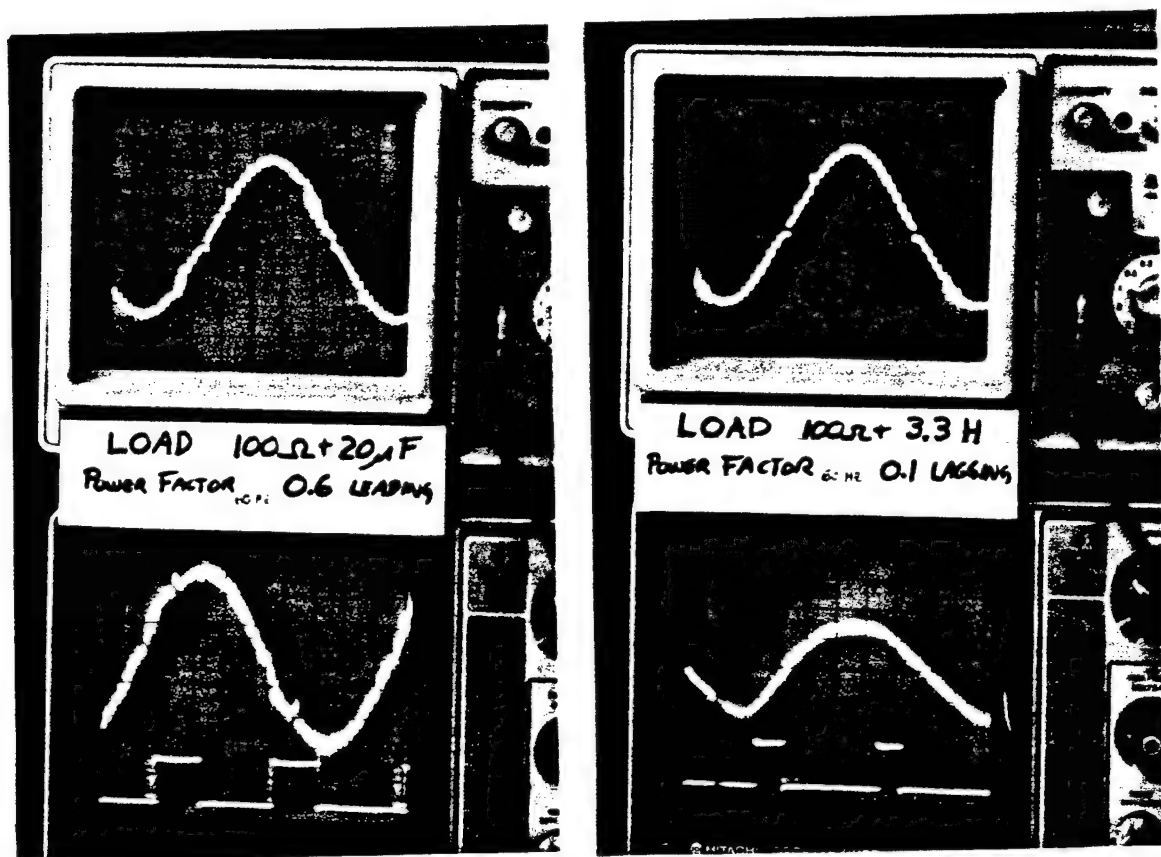


**FIGURE 26**

Reactive Loads: Waveforms With Reaction Branch  
Source: Automotive style alternator modulated at 60 Hz.  
Left: capacitive series load, Power Factor 0.6 leading  
Right: inductive series load, Power Factor 0.1 lagging  
Upper Traces: Differential load voltage at 10 V/div; Time 2ms/div  
Middle Traces: Load Current at 50 mA/div (left) and 20 mA/div (right)  
Lower Traces: Reaction Branch Gate Trigger at 10 V/div

4.6 Results of Analytical Development The sketch design for scaling the high frequency alternators up to 6 kW of 120 VAC (60 Hz) indicated that the use of a magnetic path made entirely of laminated electrical steel would reduce the field excitation losses so that the scheme would become practical. The 60 Hz core losses in the field were estimate to only 22 watts. The Q of a resonant drive system was estimated to be 37, which implies that a 12 V<sub>RMS</sub> drive signal could be amplified in the resonant tank circuit to drive the field coil at 440 V<sub>RMS</sub>. Further results are listed here:

constraints set:

V<sub>t</sub> - (set at 440V)  
 B<sub>max</sub> - (set at 1.87 T)  
 var - (set at 0.5)  
 N<sub>2</sub> - (set at 5 turns)

established by calculations:

N<sub>1</sub> - 263 turns  
 I<sub>t</sub> - 3.8 A<sub>RMS</sub> (total)  
 L<sub>t</sub> - 0.307 H (total)  
 g - 2.0 E-3 m  
 A<sub>nom</sub> - 2.0 E-3 m<sup>2</sup> per pole  
 P<sub>60</sub> - 0.14 (watts/lb) from 60 Hz Modulation of Coil  
 P<sub>800</sub> - 7.6 (watts/lb) from 800 Hz interphase alternations

Minimum magnetic core volume 780 cm<sup>3</sup>/pole  
 Density of magnetic core 7.65 g/cm<sup>3</sup>  
 Core weight per pole 5.97 kg/pole  
 Total core weight (12 poles) 71 kg (157 #)  
 Core loss/ pole 60 Hz 1.8 watts/pole  
 Core loss/ pole 800 Hz 50 watts/pole (no load)  
 100 watts/pole (with rated load current)  
 Total Core loss see by field 22 watts @ 60 Hz  
 Core loss equivalent admittance 35 k-ohm in parallel with coil  
 Q of Resonant drive 37 includes estimated losses for copper  
 V<sub>s</sub> required drive voltage 12 V<sub>RMS</sub>

These are encouraging results that make the scheme appear to be practical. The weight and losses are quite sensitive to the maximum flux density allowed, and this calculation has erred on the side of lowering losses and ignoring the weight issue. It makes no pretense at finding an optimum. It demonstrates that the alternators can be scaled up to 120V<sub>RMS</sub> and that core losses in the field coil do not need to limit the practicality of this scheme.

It should be noted that the core loss/pole at 800 Hz is 50-100 watts, or a total of 600 watts to 1.2 kW depending upon the load current. These are not unreasonable figures. They reflect the efficiency limitations of any high frequency alternator and are not particular to the 60 Hz modulation scheme. The 22 watt core losses in the field are trivial compared to the projected 6 kW output. Except for the silicon losses in the H-Bridge used for commutation of the load, the efficiency of this alternator approaches that of a alternator used for DC power generation.

Critical to this conclusion is the use of a resonant drive to power the field coil and to store the field energy as it is periodically modulated.

It is certain that a practical machine would not be as attractive as this idealized machine. The primary differences would be the effect of stray inductances and the additional (magnetically inessential) metal associated with the magnetic path.

## 5. CONCLUSIONS

5.1 General Conclusions The scheme of generating single phase 60 Hz AC power directly from high frequency alternators by modulating and commutating the output has been demonstrated. The scheme appears to have potential for straightforward development into a practical source of 60 Hz AC power.

Existing high frequency alternators, designed for DC (rectified) power, are not suitable for practical AC power generation. This is due to the core losses in modulating the field magnetic circuit at 60 Hz. Existing alternators have magnetic paths with solid cores, optimized for DC power. The core losses in the fields of these machines consume more electrical energy than is produced by the device. Calculations indicate that these core losses could be reduced to trivial levels through the use of laminated materials throughout the magnetic path.

Calculations also indicate that new alternators with better magnetic paths could be designed to be practical sources of 120 VAC (50-60 Hz) power. The study identified no significant losses other than the high frequency core losses inherent in any high frequency alternator, and the expected losses in the rectification diodes. Power electronics are used only for the usual rectification of the alternator output, for soft switching during the commutation of load, and for modest field power manipulation. All of these are easily within the state of the art.

Preliminary tests of an alternative commutation scheme to eliminate the usual H-Bridge and its silicon losses appear promising. Replacing the six usual rectification diodes with twelve SCRs appears to be a possible method to simplify the commutation scheme while increasing system efficiency, and possibly increasing the robustness of the system. If true this approach would yield an AC machine approaching the efficiency of an alternator providing DC power.

### 5.2 Recommendations

5.2.1 General Recommendations Further development work is warranted. Construction and testing of an engineering prototype for a scaled up alternator could be used to confirm the trends suggested in the calculations. There are no apparent obstacles to scaling the output to 120V, but the proposed resonant drive needs to be proven and dynamic control of the resonant drive may be challenging. The degree of reduction of 60 Hz core losses by use of laminated materials for the field's magnetic path needs to be verified.

Further development work is also warranted for the alternate commutation scheme using twelve SCRs. This could be done using existing alternators to prove this promising concept.

5.2.2 Path Toward Commercial Development There are three major technical steps on the path toward commercial development. The first is the development of an engineering prototype to characterize how a full scale machine would operate, as mentioned above. The second step would involve parametric studies to determine the effect of design options to

increase power density, decrease size and weight, or increase efficiency. These items are intimately interconnected and control the competitive merits of this approach as compared to other approaches of generating 60 Hz AC power. The final (technical) step would be development of a specific design based on market demands and manufacturing, reliability, and servicing considerations.

In parallel with the technical development, commercial development will require a marketing assessment. The power levels, size, weight and cost targets required by the market place, and the strengths of competitive devices need to be understood in order to develop the commercial potential of this approach. Because this scheme is relatively straight forward and works at a level common to all power systems employing high frequency alternators, it would seem that this approach should be very competitive if developed.

APPENDIX A  
Detailed Circuit Diagrams

APPENDIX A - SHEET 1 OF 6  
HIGH LEVEL SCHEMATIC: POWER AND CONTROL CIRCUITS

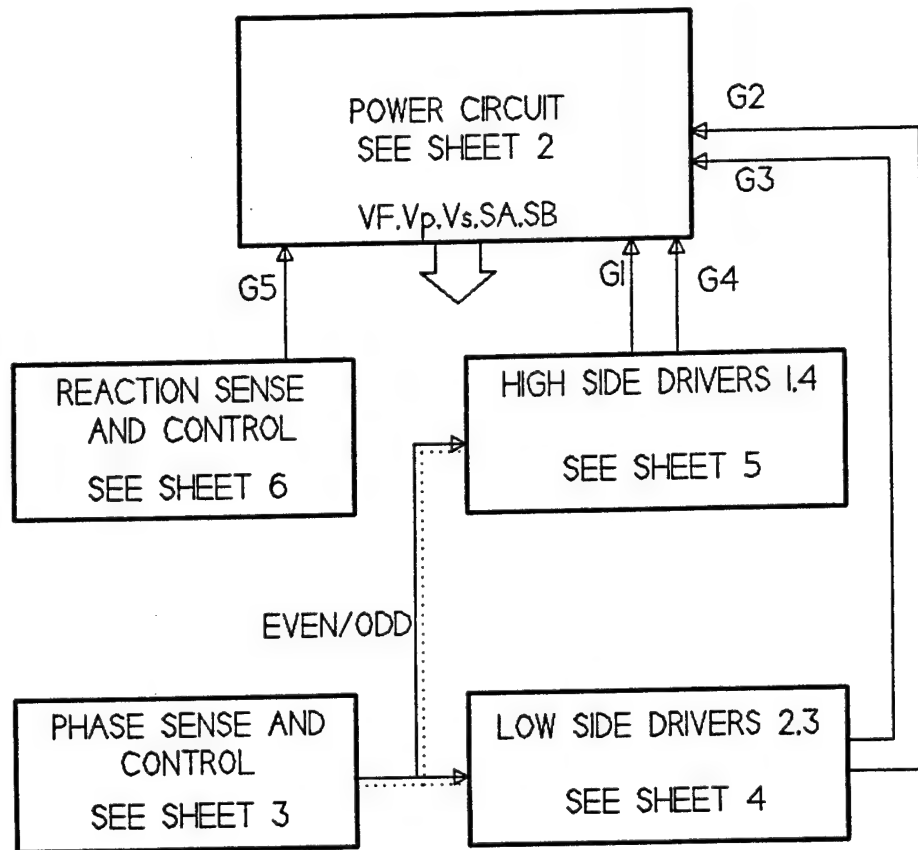


**FIGURE A-1**  
High Level Schematic: Power and Control Circuits

APPENDIX A - SHEET 2 OF 6  
POWER CIRCUIT

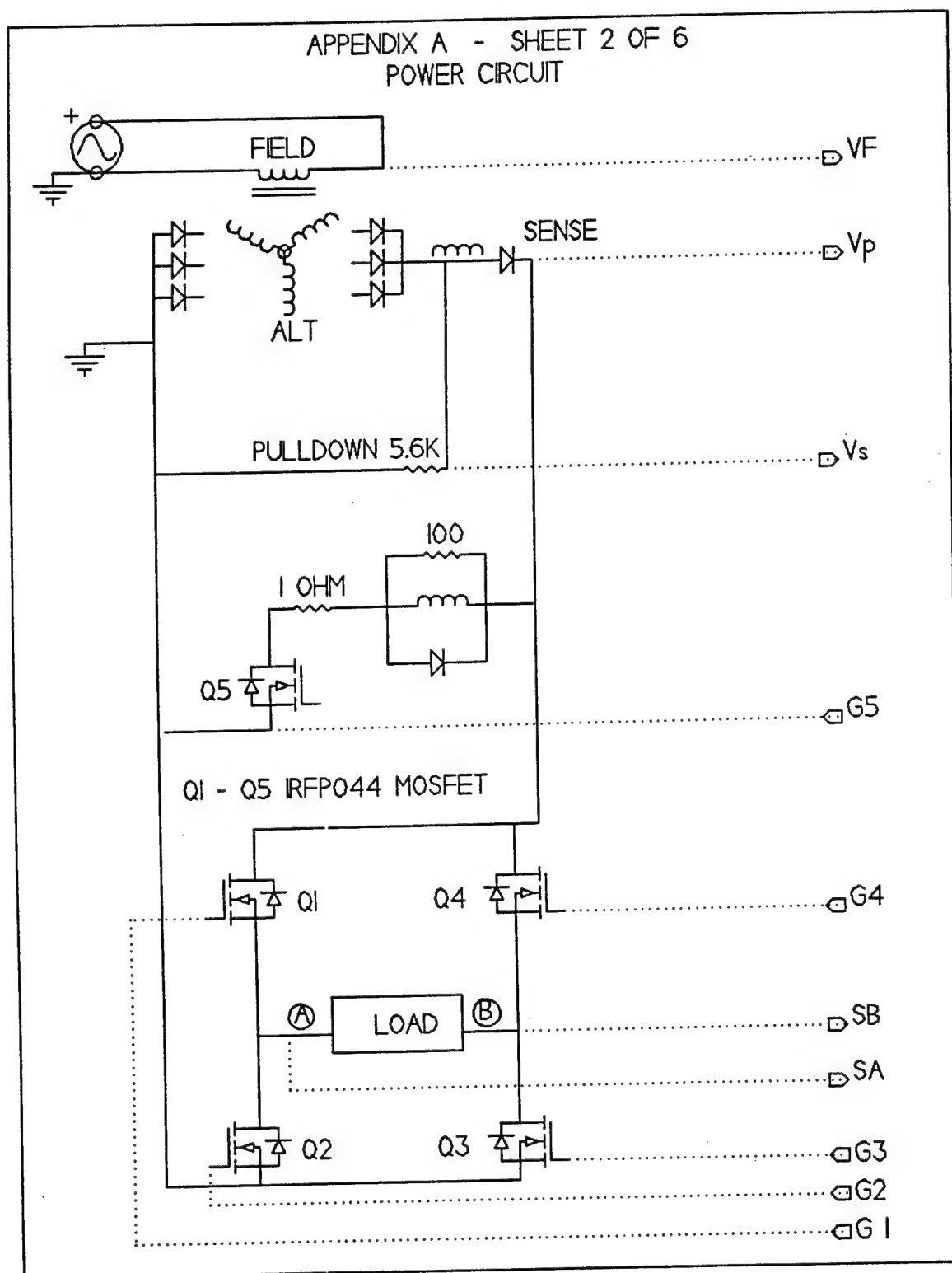


**FIGURE A-2**  
Power Circuit



APPENDIX A - SHEET 3 OF 6  
PHASE SENSE AND CONTROL

The diagram illustrates a phase sense and control circuit. It features a 5 DEGREE LEAD network consisting of three op-amp stages (347) and a 4013 flip-flop. The input is a 120 VAC REF signal, which is also connected to a 7 VOLT REF. The circuit includes various resistors (100K, 10K, 68K, 20K, 2.2K, 10K, 13K, 68K) and capacitors (3.3nF, 220pF). A 9V battery is connected to the circuit. The output of the 4013 flip-flop is labeled ODD and EVEN, with waveforms shown for each.

44

APPENDIX A - SHEET 4 OF 6  
LOW SIDE DRIVERS (2 & 3)

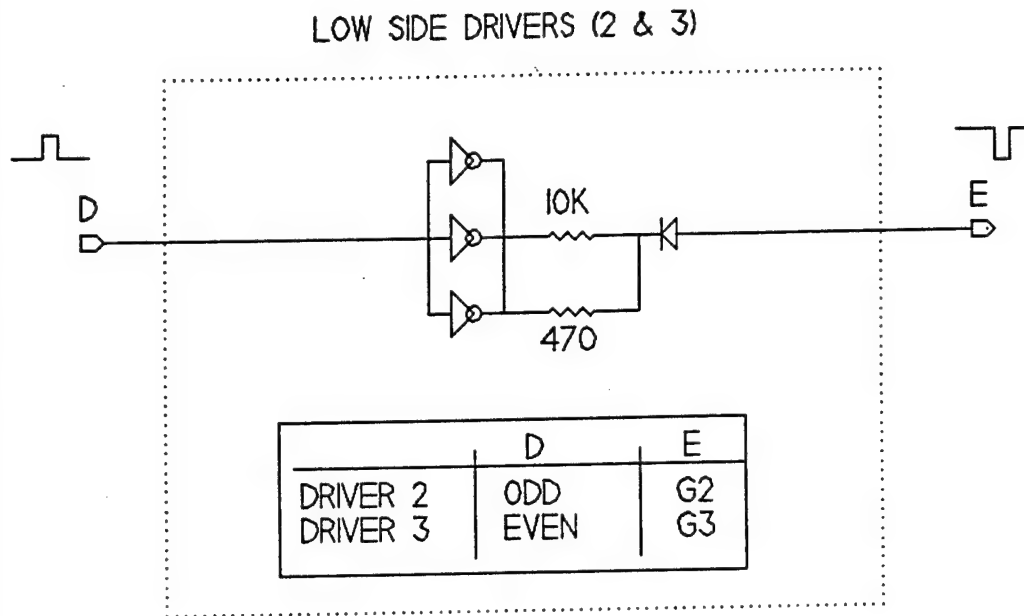


**FIGURE A-4**  
Low Side Driver Circuit

APPENDIX A - SHEET 5 OF 6  
HIGH SIDE DRIVERS (1 & 4)

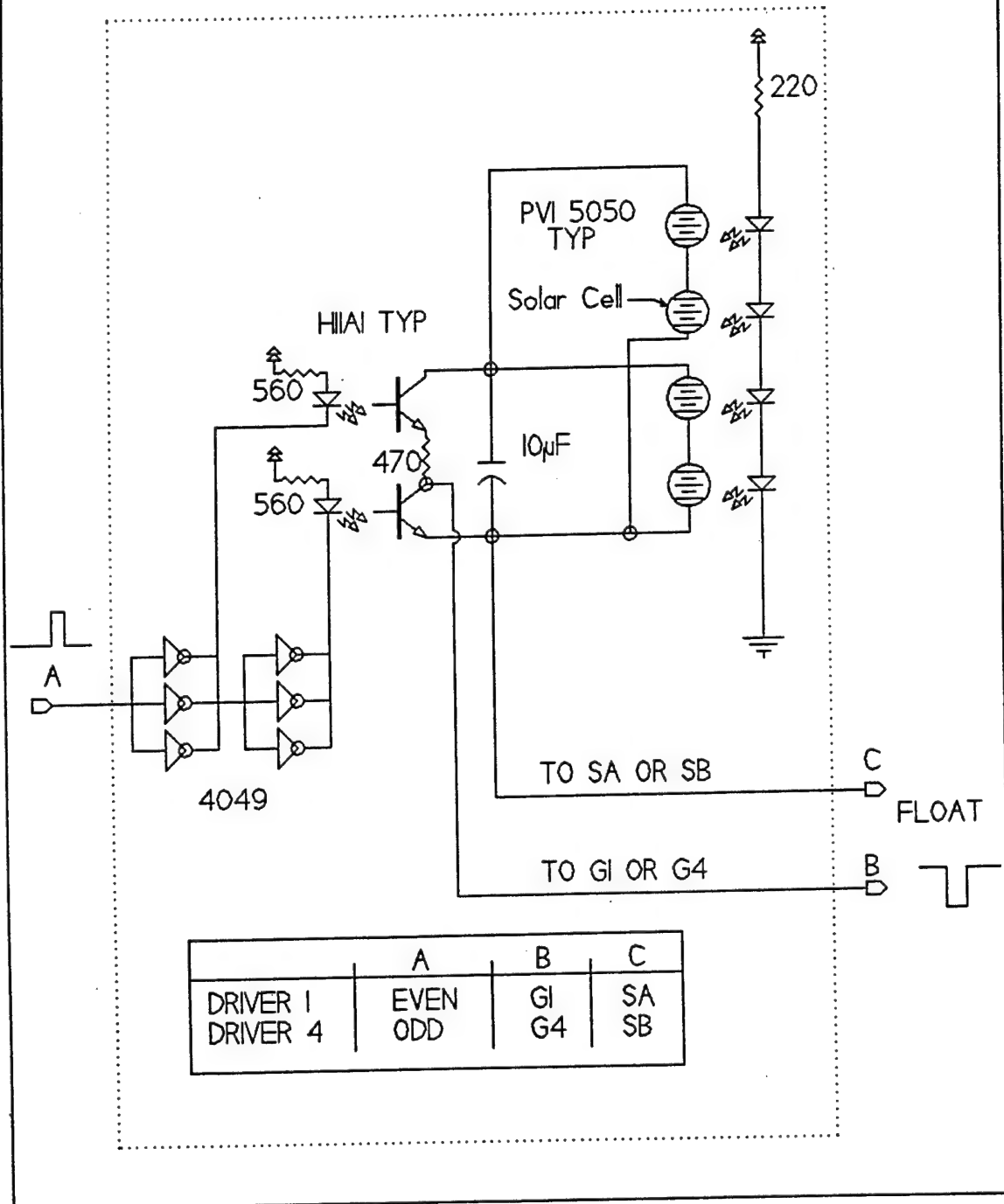


**FIGURE A-5**  
High Side Driver Circuit

APPENDIX A - SHEET 6 OF 6  
REACTION SENSE AND CONTROL

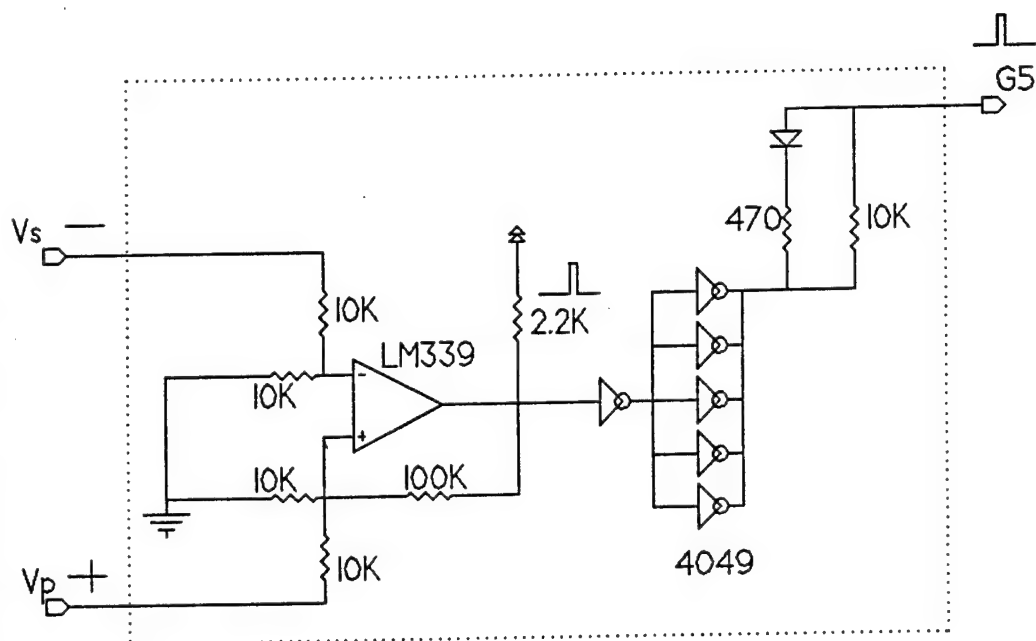


**FIGURE A-6**  
Reaction Sense and Control Circuit

APPENDIX B  
CALCULATION FOR SKETCH DESIGN  
120 VAC, 6KW 60HZ

SECTION 1  
INTRODUCTION

This calculation determines the core size and coil turns needed for a high frequency alternator generating 6KW of 120VAC 60 Hz power through modulation of the field and commutation of the load. It envisions a magnetic path made entirely of laminated electrical steel.

For ease of calculation this analysis assumes a three phase alternator producing a hex phase rectified ripple pattern. The magnetic flux variation is assumed to be accomplished by the rotational variation of the cross sectional area of a fixed length air gap. Figure B-1 shows how this variation works. The magnetic flux is assumed to be controlled by the air gap (that is, for this first approximation the reluctance of the metal core is ignored.) In a practical machine the core reluctance would be of some importance. Also in a practical machine it might be more convenient to accomplish the flux variation by rotational changes in the air gap length instead of the air gap cross sectional area.

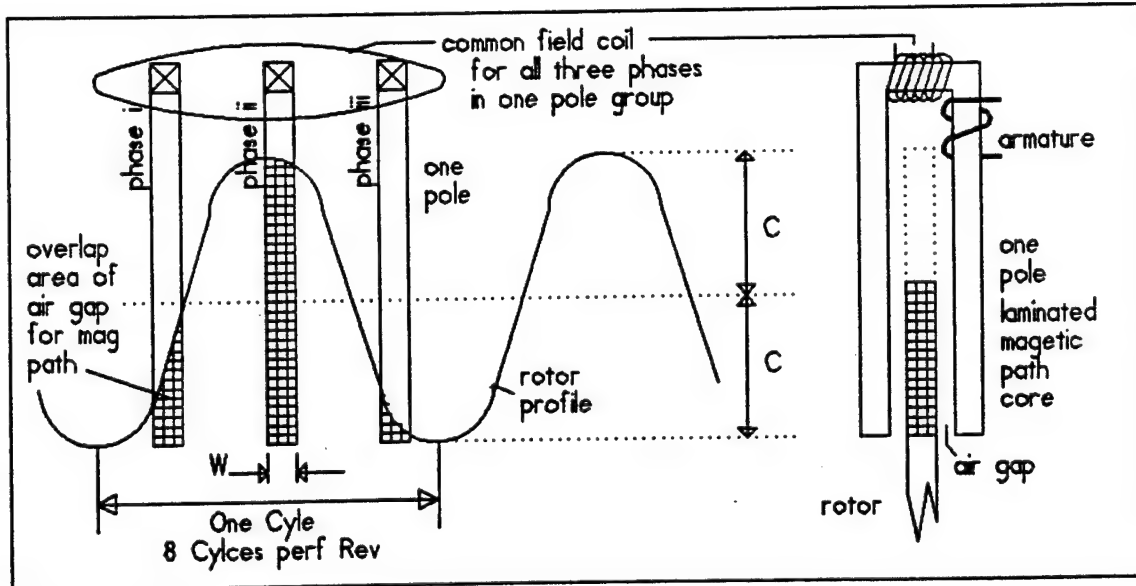


Figure B-1  
Air Gap Area Variation

For this machine we will assume that there are eight sine wave cycles per revolution, as suggested in Figure B-1.

TABLE B-1  
List of Variables

A	core cross section area, nominal	m <sup>2</sup>	
W	width of airgap cross section	m	
C	amplitude of airgap length variation	m	
$\omega$	frequency of airgap variation	rad/s	
t	time	sec	
Vp	Peak output voltage	v	
Vt	total field drive voltage	v	
It	total field drive current	a	
I1	field drive current per winding	a	
I2	output current per winding	a	
et	rectified output voltage, total	v	
ex	phase voltage, gen x, phase i,ii,iii	v	
ep	pole voltage	v	
$\Phi$	flux	webers	
Lt	inductance, total field coil	henries	
L	inductance, one pole group (field coil)	henries	
N1	field coil turns	turns	
N2	armature coil turns	turns	
$\mu$	free space permeability	H/m	
g	air space gap length	m	
$\omega_{60}$	frequency of 60Hz field modulation	rad/sec	
turnratio	N1/N2		
VAR	variation in Pole MMF due to I2		
d $\Phi$ /dt	time derivative of flux	weber/s	
FLUXMAX	Nominal amplitude- 60 Hz flux density	tesla	
Coreloss60	Eddy current losses @ 60Hz	watts	
Coreloss800	Eddy current losses @800Hz	watts	

From convolution simulations we have found that the air gap cross section of each pole in Figure B-1 remains at:

$$\text{AREA} \sim C \cdot W \cdot \{1 + \sin(\omega \cdot t + \alpha)\} \text{ as long as } (W < \pi/2.) \quad \text{EQUATION 1}$$

Then we can calculate the frequency of flux change as:

$$\text{RPM} := 6000 \quad (\text{assumed})$$

$$\omega := (\text{RPM} \cdot 8) \cdot 2 \cdot \frac{\pi}{60} \quad \text{rad/sec, based on 8 cycles/rev}$$

$$\omega = 5.027 \cdot 10^3 \quad \text{rad/sec}$$

also we have the 60 Hz modulation:

$$\omega_{60} := 2 \cdot \pi \cdot 60 \quad \text{rad/sec}$$

$$\omega_{60} = 376.991$$

A single pole group in this machine is wired with one pole for each of the three phases, all having a common field winding, as shown in Figure B-1. The entire winding scheme is shown in the text in Figure 17. Because of this arrangement the total air gap area for the pole group is the sum of three sinusoids of Equation 1, each displaced by 120°. This means that the total area is:

$$A_{\text{total}} = 3 \cdot C \cdot W,$$

regardless of rotor position. This also means that the inductance seen by the field coil is constant although flux shifts among the poles of the group with rotation; The total flux of the group is constant.

Figure B-2 shows the arrangement of armature coils. The maximum output voltage will be as the two conducting phases are each at 30 degrees from their respective peaks, as shown. This can be verified by constructing three phase rectified output as shown in Figure 1 of the text. The ripple voltage has a rectified average at 0.95 times this peak value.

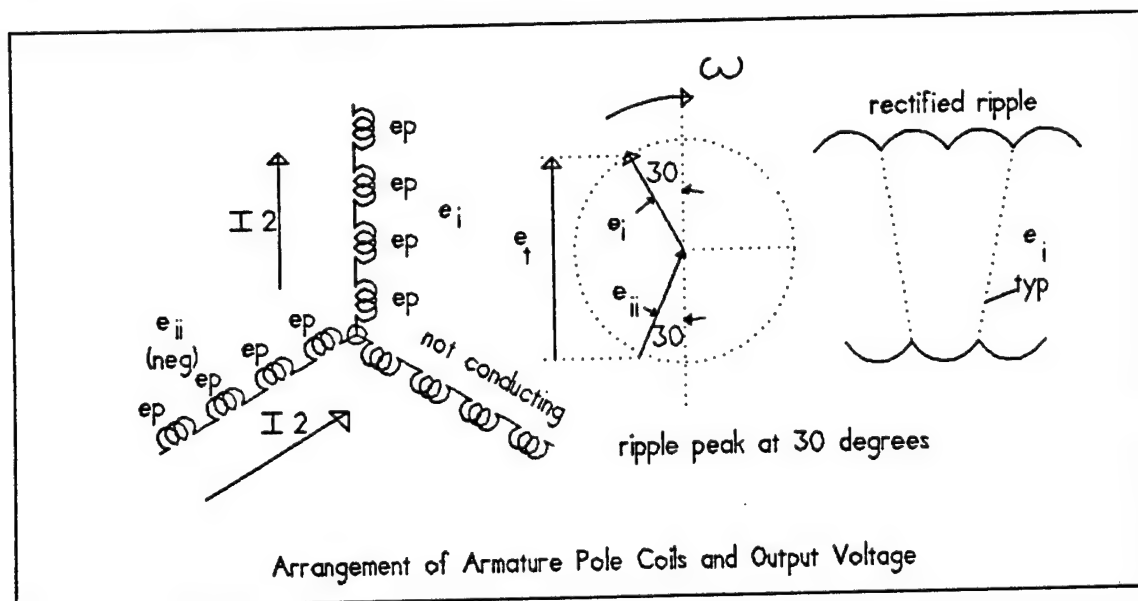


Figure B-2  
Armature Coils - Voltage

For 120VAC output we need an (rectified averaged) output peaking at  $(1.41 \cdot 120)$  volts. This gives, 169 volts and is 0.95 times the ripple peak (178 volts). We must further allow for a couple of diode drops, say 3 volts total, so the needed peak output ripple voltage is:

$$e_t := \frac{120 \cdot \sqrt{2} \cdot \text{volt}}{.95} + 3 \cdot \text{volt} \quad e_t = 181.638 \cdot \text{volt}$$

$$\text{at maximum} \quad e_{t_{\max}} = (0.866 e_{x_{\max}}) - (-0.866 e_{x_{\max}}) = 1.73 \cdot e_{x_{\max}}$$

$$e_x := \frac{e_t}{1.73} \quad e_x = 104.993 \cdot \text{volt}$$

Figure B-2 showed that the sense of  $I_2$  is opposite for phases (ii) and (i). The influence of  $I_2$  will change the flux and lower  $e_i$  but will increase  $e_{ii}$  and  $e_t$  will stay constant. Within  $e_x$  there are four series poles  $e_p$  each at  $1/4$  the total  $e_x$ .

$$e_p := \frac{e_x}{4}$$

$$e_p = 26.248 \text{ volt}$$

This is the nominal peak pole voltage without corrections for  $I_2$ . Corrections for  $I_2$  are not yet needed because (1) at no load  $I_2=0$ , and (2) with load,  $I_2$  causes interpole variations from the nominal, but the total effect is nil. (This is not true if losses from leakage flux, magnetic saturation, eddy currents and copper losses are taken into account, but the "no load" machine provides a nominal starting point.)

Because of the arrangement of the field coils (see text Figure 17

$$\mu_0 := 4 \cdot \pi \cdot 10^{-7} \frac{\text{henry}}{\text{m}}$$

If  $L_t$  is the total inductance

$$L_t := \frac{V_t}{2 \cdot \pi \cdot 60 \cdot I_t} \text{ henry}$$

from  $Z=V/I$ , and from above:  $L_t := L$

Also:

$$L := \frac{N^2 \cdot 3 \cdot C \cdot W \cdot \mu_0}{g}$$

from the formula for inductance of an air gap, with area  $3 \cdot C \cdot W$



Table B-2

OUTLINE OF CALCULATION

- 1 Notes on machine type (above)
- 2 temporarily set  $I_2=0$   
write  $\Phi(t)$   
find  $d\Phi/dt$   
find  $d\Phi/dt$  max
- 3 from  $e_p = N_2 \cdot (d\Phi/dt)$  derive  $N_1/N_2$   
set  $N_2$ , find  $N_1$
- 4 Set acceptable max flux variation due to  $I_2$   
( $I_2$  at desired 50 AMPS rms)  
Find, then, required  $I_1$
- 5 From  $I_1$  calculate  $L$
- 6 Set maximum allowable flux density  
find then required  $g$
- 7 From  $g$  and  $L$  calculate air gap area ( $C \cdot W$ )
- 8 Map into physical dimensions
- 9 Calculate  $\Phi(t)$
- 10 Figure Hysteresis losses

SECTION 2

CALCULATION OF  $d\Phi/dt$

$$i_1(t) := I_1 \cdot \sin(\omega t) \quad (\omega 60 \text{ also noted as } 377 \text{ rad/sec})$$

$$\Phi(t) := (N_1 \cdot i_1(t) + N_2 \cdot I_2) \cdot \frac{\mu_0}{g} \cdot C \cdot W \cdot (1 + \sin(\omega t)) \quad \{\text{This is for one pole only}\}$$

For convenience define  $K$ : 
$$K := \frac{N_1 \cdot \mu_0 \cdot C \cdot W \cdot I_1}{g}$$

Let  $I_2=0$  (temporarily), so

$$\Phi(t) := K \cdot \sin(377 \cdot t) \cdot (\sin(\omega \cdot t) + 1) \quad \text{and then let } d\Phi/dt \text{ be noted } d\Phi/dt$$

$$d\Phi/dt := 377 \cdot K \cdot \cos(377 \cdot t) + (377 \cdot K \cdot \cos(377 \cdot t) \cdot \sin(\omega \cdot t) + \omega \cdot K \cdot \sin(377 \cdot t) \cdot \cos(\omega \cdot t))$$

$d\Phi/dt$  will be maximum at  $\sin(377 \cdot t)=1$ , due to large  $\omega$ ,  
and then  $\cos(377 \cdot t)=0$ , so:

$$d\Phi/dt := \omega \cdot K \cdot \cos(\omega \cdot t) \quad \text{is the max, which then has its temporal max at}$$

$$d\Phi/dt := \omega \cdot K$$

### SECTION 3

Now from  $e_p = N_2 \cdot (d\Phi/dt)$  we calculate  $N_1/N_2$ :

$$e_p := N_2 \cdot \omega \cdot K \quad \text{and} \quad K := \frac{N_1 \cdot C \cdot W \cdot I_1 \cdot \mu_0}{g}$$

$$\text{so,} \quad e_p := N_2 \cdot \omega \cdot \left( \frac{N_1 \cdot C \cdot W \cdot I_1 \cdot \mu_0}{g} \right)$$

and we know from above:

$$L_t := \frac{V_t}{(\omega 60) \cdot I_t} \cdot \text{henry}$$

$$\text{and } I_t = 2 \cdot I_1$$

$$L := \frac{N_1^2 \cdot 3 \cdot C \cdot W \cdot \mu_0}{g}$$

so we can rewrite:

$$e_p := \frac{N_2}{N_1} \cdot \left( \frac{\omega}{3 \cdot 2 \cdot \omega 60} \right) \cdot V_t$$

Interestingly, this is the transformer equation adjusted by the ratio of the frequencies. This makes sense. Now let us set  $V_t = 440\text{v RMS}$  as a practical maximum driving voltage for the 60 Hz resonant drive. Then the peak  $V_t$ :

$$V_t := 440 \cdot \text{volt} \cdot \sqrt{2}$$

$$V_t = 622.254 \cdot \text{volt}$$

$$\omega 60 = 376.991$$

$$e_p := \frac{e_x}{4}$$

$$e_p = 26.248 \cdot \text{volt}$$

$$\omega = 5.027 \cdot 10^3$$

$$\text{so } N_1/N_2 = \text{turnratio} := \left[ \frac{e_p}{V_t} \cdot \left[ \frac{3 \cdot 2 \cdot (\omega 60)}{\omega} \right] \right]^{-1}$$

$$\text{turnratio} = 52.681 = N_1/N_2$$

#### SECTION 4

From acceptable levels of flux change due to  $I_2$ , calculate  $I_1$ .

As shown in Figure B-3, as the cross sectional area of the air gap changes, the conduction period causes a change in the flux level due to reverse MMF from  $(I_2 \cdot N_2)$ . The relative size of this change depends upon  $(I_1 \cdot N_1)$ , since the total MMF in the pole is  $(I_1 \cdot N_1 + I_2 \cdot N_2)$ . In poles where the sense of  $I_2$  adds to the MMF of  $I_1$ , then the peak flux is increased, increasing eddy current losses. Also, in the extreme, the peak flux starts into the magnetic saturation range, increasing losses. This can be minimized by using a large  $(I_1 \cdot N_1)$ , but this has consequences of increasing the copper and the induction of the coil.

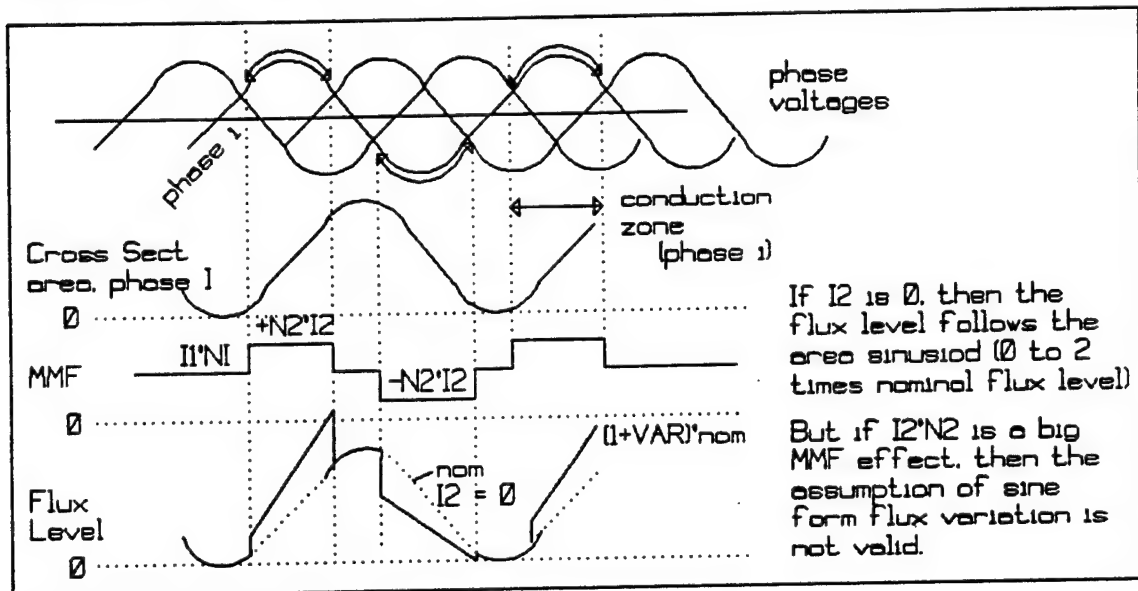


Figure B-3  
Flux Variation

Let us define VAR to be the change of total MMF in the pole air gap as  $I_2$  is increased from zero to full value. Then:

$$(N_1 \cdot I_1 + N_2 \cdot I_2) = (1 + \text{VAR}) \cdot N_1 \cdot I_1$$

or  $I_1 = (N_2 / N_1) \cdot (1 / \text{VAR}) \cdot I_2$

$$I_2 := 50 \cdot \text{amp} \cdot \sqrt{2}$$

$$I_2 = 70.711 \cdot \text{amp}$$

$$\text{VAR} := 0.5$$

(set arbitrarily)

$$I_1 := (\text{turnratio} \cdot \text{VAR})^{-1} \cdot I_2$$

from above, so:

$$I_1 = 2.684 \cdot \text{amp}$$

$I_1$ , peak

$$I_t := 2 \cdot I_1$$

$$I_t = 5.369 \cdot \text{amp} \text{ (} I_t \text{ peak, )}$$

$$\frac{I_t}{\sqrt{2}} = 3.796 \cdot \text{amp RMS}$$

## SECTION 5

Knowing  $I_1$ , now calculate the field coil inductance  $L$ :

$$L_t := \frac{V_t}{(\omega 60) \cdot \sec^{-1} \cdot I_t}$$

$$L_t = 0.307 \cdot \text{henry}$$

$$L := L_t$$

$$L = 0.307 \cdot \text{henry}$$

## SECTION 6

Now calculate the required gap  $g$  to establish the needed limit on  $\Phi/A$ , flux density

For a first try we will limit the induction to near 10 kgauss. (10 kgauss = 1 tesla = 1weber/m<sup>2</sup>) {Actually we limit the nominal inductance (FLUXMAX) to 6.7 kgauss so that the maximum high frequency inductance  $(1+VAR) \cdot (1+\sin(60))$  will be less than 18.7 kgauss, which is near saturation. See the flux density peaks in Figure B-3.}

Furthermore, we set a minimum number of turns for  $N_2$  in order to have an efficient coil.

$$N_2 := 5$$

set arbitrarily

$$N_1 := N_2 \cdot \text{turnratio}$$

$$N_1 = 263.406$$

$$\text{FLUXMAX} := 0.67 \cdot \text{tesla}$$

(Nominal Maximum Flux)

$$g := (N_1 \cdot I_1 + N_2 \cdot I_2) \cdot \frac{\mu_0}{\text{FLUXMAX}}$$

from  $\Phi/A = \text{MMF} \cdot \mu_0 / g$ , for air gap with all MMF in air gap

$$g = 0.002 \cdot \text{m}$$

air gap length

## SECTION 7

From known gap length and inductance, calculate the nominal cross sectional area  $A=C \cdot W$

$$L := \frac{N^2 \cdot 3 \cdot C \cdot W \cdot \mu_0}{g}$$

$$A := C \cdot W$$

$$A := \frac{L \cdot g}{3 \cdot N^2 \cdot \mu_0}$$

$$A = 0.002 \cdot m^2$$

cross section area of gap and core,  
nominal

$$\sqrt{A} = 0.048 \cdot m$$

basic dimension of square cross section,  
48 mm

$$\sqrt{A} = 1.904 \cdot in$$

or 2" \* 2"

## SECTION 8

Plotting the cross sectional area of each core element into the rough sketch of Figure B-4, we arrive at a volume of approximately 780 cm<sup>3</sup>/pole. There are 12 such poles. The density of the laminated material is 7.65g/cm<sup>3</sup>.

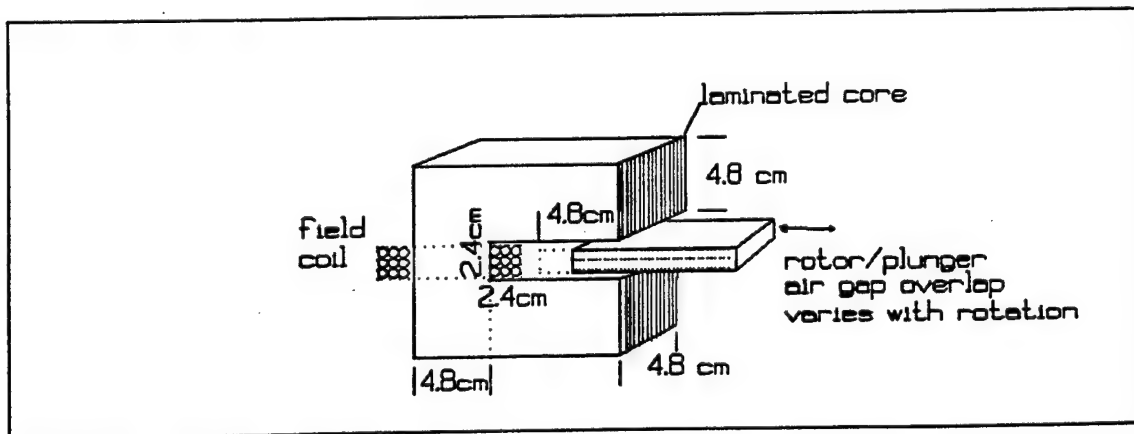


Figure B-4  
Sketch of Pole Core Dimensions

Now calculate the weight of the 12 cores as sketched:

$$\text{Vol} := 780 \cdot \text{cm}^3$$

$$\text{Density} := \frac{7.65 \cdot \text{gm}}{\text{cm}^3}$$

$$\text{WGT} := 12 \cdot \text{Vol} \cdot \text{Density}$$

$$\text{WGT} = 71.604 \cdot \text{kg}$$

$$\text{WGT} = 157.86 \cdot \text{lb}$$

### SECTION 9

$$I_i(t) := I_1 \cdot \sin(\omega 60 \cdot t)$$

Now we calculate the Flux variation with time: Nominally:

$$\Phi(t) := (N_1 \cdot I_i(t) + N_2 \cdot I_2) \cdot \frac{\mu_0}{g} \cdot C \cdot W \cdot ((1 + \sin(\omega \cdot t)))$$

Due to the conduction periods ( $I_2$  not equal to 0) shown back in Figure B-3, the last term (the 800 Hz variation) has a maximum at ( $\omega \cdot t = 60$  degrees), so the 800 Hz variation in flux is assymmetrical, from zero to  $\Phi(\text{max})$ , where:

$$\Phi(\text{max}) := (N_1 \cdot (1 + \text{VAR}) \cdot I_{1\text{max}}) \cdot \frac{\mu_0}{g} \cdot C \cdot W \cdot ((1 + 0.866))$$

and this is modulated at 60 Hz, as shown in Appendix C. This can be rewritten:

$$\Phi_{800} = 1.875 \cdot \text{tesla}$$

Note  $\Phi_{800}$  is the maximum peak to peak varitation of the flux level and not the 800 Hz amplitude.

## SECTION 10

### CALCULATION OF CORE LOSSES

As discussed in Appendix C, the core loss can be divided into two frequency components, one at the 60 Hz field modulation frequency which influences the field excitation, and one at the high (800 Hz) ripple frequency which influences the shaft power and the output.

The field core losses at 60 Hz are unique to the modulated alternator. They are independent of load current and can be calculated as follows:

$$\text{Coreloss60} := 0.31 \cdot \text{FLUXMAX}^2 \cdot \frac{\text{watt}}{\text{lb} \cdot \text{tesla}^2} \cdot \text{WGT}$$

$$\text{Coreloss60} = 21.968 \cdot \text{watt}$$

The armature core losses at 800 Hz are common to all alternators working at this frequency and flux level. They can be calculated as follows:  
{Note that we use one half of  $\Phi_{800}$  in order to get the amplitude (1/2 the peak to peak value) of the instantaneous flux variation.}

$$\text{Coreloss800} := \left( \frac{17.0}{2} \right) \cdot \left( \frac{\text{watt}}{\text{lb} \cdot \text{tesla}^2} \right) \cdot \left( \frac{\Phi_{800}}{2} \right)^2 \cdot \text{WGT}$$

$$\text{Coreloss800} = 1.18 \cdot 10^3 \cdot \text{watt}$$

Note: this core loss is based on carrying the full load current and would be less for lower current conditions.

It is to be expected that a practical machine would not be as attractive as the sketch design presented in this calculation. This calculation has ignored the MMF required by the metal core and leakage inductance and copper losses.

## APPENDIX C

### OUTLINE OF CORE LOSS ESTIMATION PROCEDURE

It is desired to estimate the core loss in a proposed machine where the core inductance is described by :

$$B_c(t) = B' \sin(377t) * [1 + \sin(5026t)], \text{ where}$$

$t$  is time  
 $B_c(t)$  is variation of core flux with time  
 $B'$  is peak flux amplitude (nominal)  
 $(377t)$  represents 60 Hz cycling  
 $(5026t)$  represents 800 Hz cycling

Graphically, this time variation of flux is shown in Figure C-1. Physically this is result of exciting the machine with a 60 Hz AC field and then changing the core flux with a moving air gap.

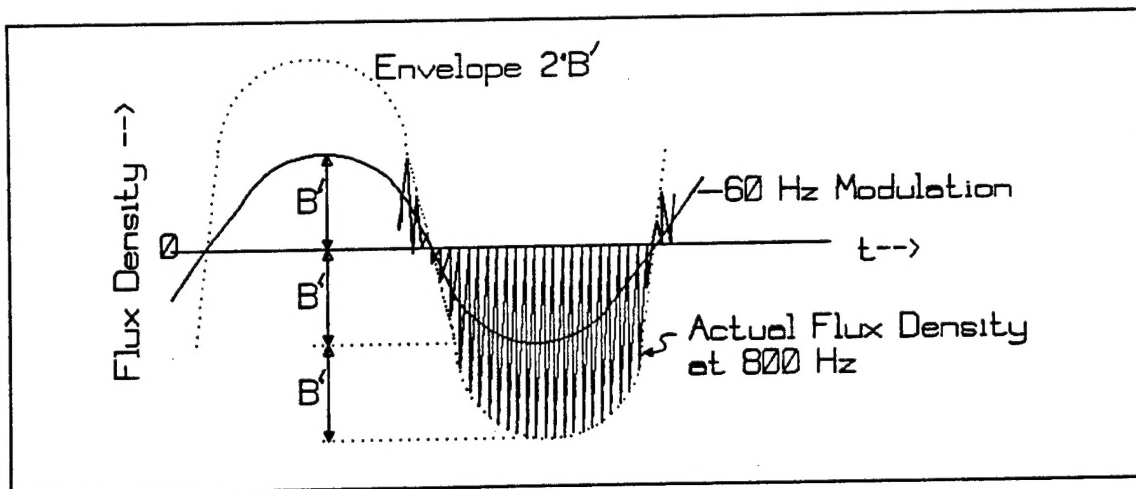


**FIGURE C-1**  
Time Modulation of Core Flux for Sketch Design

This excitation produces a temporarily non symmetrical 800 Hz flux pattern that varies from 0 to  $2*B'$  (peak to peak). This pattern is then reversed by 60 Hz modulation to complete the symmetry.

The core losses are estimated by breaking the loss into two frequency components, (A) and (B), where:

- (A)  $Loss_{60}$  is based on  $B'$ . This loss will account for the overall reversal of the field at 60 Hz.
- (B)  $Loss_{800}$  is the average of the instantaneous 800 Hz loss, averaged over the half cycle of 60 Hz modulation.



Assumption 1 It is assumed that one can use the published data for core loss with symmetrical excitation and apply it to the offset excitation as long as the peak induction remains in the linear range (ie, below saturation.) Since eddy current losses vary as frequency squared, they tend to overshadow hysteresis losses at high frequencies. Assuming that 800 Hz represents high frequency in this context, one can note that eddy current losses are governed by  $dB/dt$  (where B is the magnetic flux density), and the average flux level is not involved. This would support this first assumption.

Assumption 2 It is further assumed that published data is based on the amplitude of induction variation. (That is, the induction values cited are one half the peak to peak variation of the induction.) For comparison see Reference 1\* figure 4-34, page 4-104.

In the machine described the amplitude of induction variation is:

Symmetrical 60 Hz:            Amplitude =  $B'$   
Asymmetric 800 Hz:           Amplitude =  $B'$

By interpolating and curve fitting the data in Reference 1, data for 30H083, grain oriented electrical steel (annealed Epstein)

$$\text{Average Core Loss}_{60} = 0.31 * (B')^2 \quad \text{watts/lb}$$

$$\frac{\text{Instantaneous}}{\text{Core Loss}_{800}} = 17 * (B_c(t))^2 \quad \text{watts/lb}$$

where  $B_c(t)$ , and  $B'$  are in Teslas (webers/m\*m)

To find the Average Core Loss<sub>800</sub>, integrate the instantaneous Core Loss<sub>800</sub> over one half cycle of the 60 Hz modulation and average it. Due to the integral of  $(\sin^2)$  from 0-PI, the average comes to be one half the peak. So:

$$\text{Average Core Loss}_{800} = (17/2) * (B')^2 \quad \text{watts/lb}$$

By this approach the total core loss should be the sum of the averages

$$\text{Total Core Loss} = 0.31 (B')^2 + (17/2) * (B')^2 \quad \text{watts/lb}$$

or

$$\text{Total Core Loss} = 8.81 (B')^2 \quad \text{watts/lb}$$

We conclude that 96 % of the core loss comes from the 800 Hz variation. For  $B' = 1$  Tesla, the core loss will be 8.81 watts/lb

---

\* Reference 1: Fink and Beaty, Standard Handbook for Electrical Engineers, 12th Ed., 1987, McGraw Hill, NY